Advanced Review

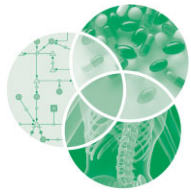

Integrative modeling of the cardiac ventricular myocyte

Raimond L. Winslow,[1]* Sonia Cortassa,[2] Brian O'Rourke,[2] Yasmin L. Hashambhoy,[1] John Jeremy Rice[3] and Joseph L. Greenstein[1]

Cardiac electrophysiology is a discipline with a rich 50-year history of experimental research coupled with integrative modeling which has enabled us to achieve a quantitative understanding of the relationships between molecular function and the integrated behavior of the cardiac myocyte in health and disease. In this paper, we review the development of integrative computational models of the cardiac myocyte. We begin with a historical overview of key cardiac cell models that helped shape the field. We then narrow our focus to models of the cardiac ventricular myocyte and describe these models in the context of their subcellular functional systems including dynamic models of voltage-gated ion channels, mitochondrial energy production, ATP-dependent and electrogenic membrane transporters, intracellular Ca dynamics, mechanical contraction, and regulatory signal transduction pathways. We describe key advances and limitations of the models as well as point to new directions for future modeling research. *WIREs Syst Biol Med*

INTRODUCTION

Cardiac electrophysiology is a discipline with a rich history, extending from the early 1960s, of experimental research coupled with integrative modeling. The goal of this modeling has been to achieve a quantitative understanding of the relationships between molecular function and the integrated behavior of the cardiac myocyte in health and disease. Some of the most fundamental advances in computational cell biology, including formulation of dynamic models of voltage-gated ion channels, mitochondrial energy production, ATP-dependent and electrogenic membrane transporters, intracellular Ca dynamics, ligand-gated receptors, and signal transduction pathways have emerged from this field. Our goal in this paper is to review the development of these models, as well as point to new directions for future modeling research.

*Correspondence to: rwinslow@jhu.edu

[1]Institute of Computational Medicine and Department of Biomedical Engineering, Johns Hopkins University, Baltimore, MD, USA

[2]Division of Cardiology, Department of Medicine, Johns Hopkins University, Baltimore, MD, USA

[3]IBM Corporation, TJ Watson Research Center, Yorktown Heights, NY, USA

DOI: 10.1002/wsbm.122

As a result of the close interplay between modeling and experiments, we have a remarkably deep understanding of cardiac myocyte function. The most fundamental property of cardiac myocytes is that they are electrically excitable cells. Rhythmic electrical activity of the heart is initiated by pacemaking cells within the sinoatrial (SA) node. Frequency entrainment of these oscillations is assured by electrical coupling of neighboring SA node cells via gap junctions.[1] This oscillatory wave of electrical depolarization propagates into and through the right and left atria, initiating atrial contraction and filling of the right and left ventricles. The depolarization wave is then conducted through cells of the atrioventricular (AV) node and the Purkinje fiber system to initiate electrical depolarization and contraction of the ventricles. A major focus of molecular cardiobiology has been to identify and model the ion transport mechanisms whose interactions give rise to the electrical excitability of cardiac myocytes. We will review modeling of these processes and will focus primarily on modeling of the cardiac ventricular myocyte.

Figures 1 and 2 show several important structural aspects of the ventricular myocyte. These are t-tubules, the network and junctional sarcoplasmic reticulum (NSR and JSR, respectively), mitochondria, and the contractile apparatus. T-tubules are

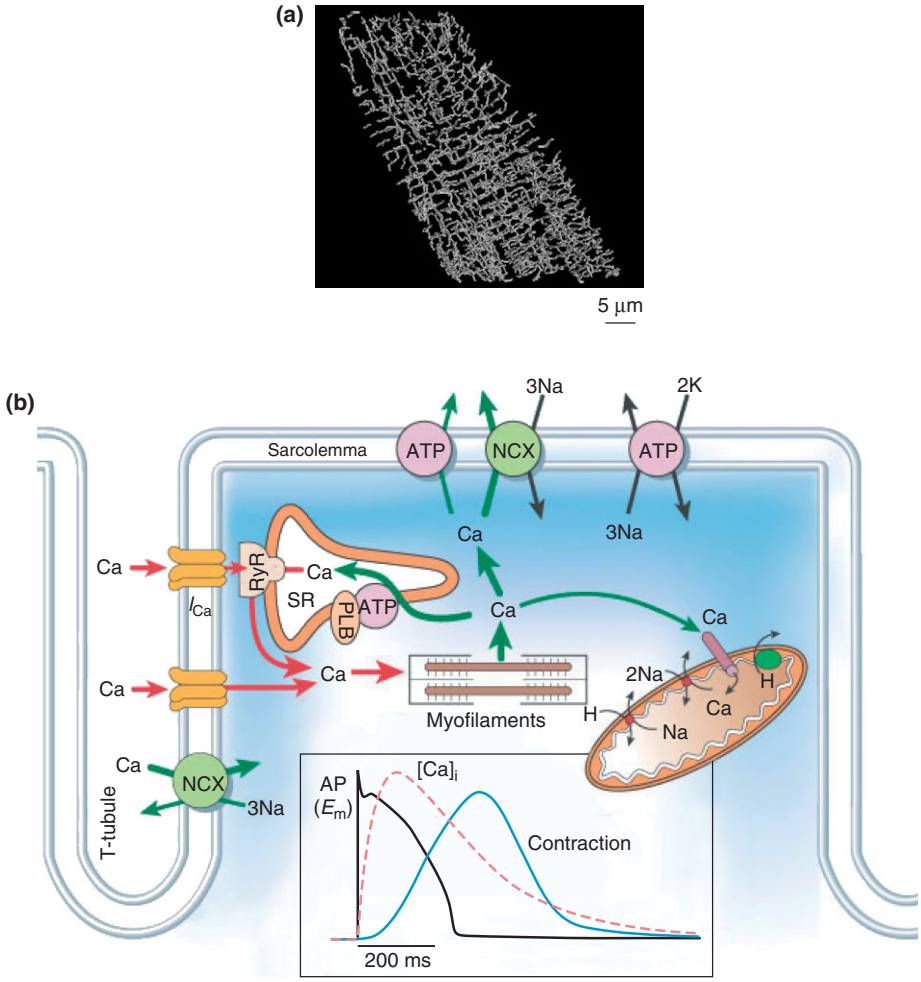

FIGURE 1 | (a) Reconstruction of the three-dimensional t-tubular system in a rat ventricular myocyte (Reprinted with permission from Ref 2. Copyright 1999 American Heart Association). (b) Ca transport in ventricular myocytes (Reprinted with permission from Ref 3. Copyright 2002 Macmillan Magazines Ltd.). Inset shows time course of action potential, Ca transient, and contraction.

invaginations of the sarcolemma extending deep into the cell. A reconstruction of the t-tubule network by Soeller and Cannell[2] is shown in Figure 1(a), and a schematic illustration of the functional organization of the t-tubule is shown in Figure 1(b).[3] The SR is a luminal organelle located throughout the interior of the cell. It is involved in uptake, sequestration, and release of Ca in a process known as intracellular Ca cycling. The JSR is the portion of the SR most closely approximating the t-tubules (Figure 1(b)), the distance between these structures being ~12–15 nm.[4] This region of close approximation is known as the dyad or the dyadic space. L-type Ca channels (LCCs) are preferentially located in the sarcolemmal portion of the dyad. The majority of the RyRs are found in the JSR directly opposed to the LCCs. When LCCs open in response to membrane depolarization, Ca flows into the dyadic space. Ca may then bind to the RyRs, inducing them to open and release Ca stored in the JSR. This process is known as Ca-induced Ca release (CICR). The resulting rise in cytosolic Ca regulates a wide range of processes including muscle contraction, properties of the cardiac action potential (AP), mitochondrial ATP production, intracellular signaling processes, and gene expression. We will review models of CICR and Ca cycling.

In cardiac myocytes, mitochondria are located near the major ATP-utilizing processes (i.e., cross-bridge cycling and muscle contraction, and pumping of Ca into the NSR). Mitochondria sense and are regulated by local levels of Ca near the dyad. Our understanding of the processes by which mitochondrial energy production is regulated in the cardiac myocyte is advancing rapidly.[6–9] We will review models of mitochondrial energy production and its coupling to membrane transport processes.

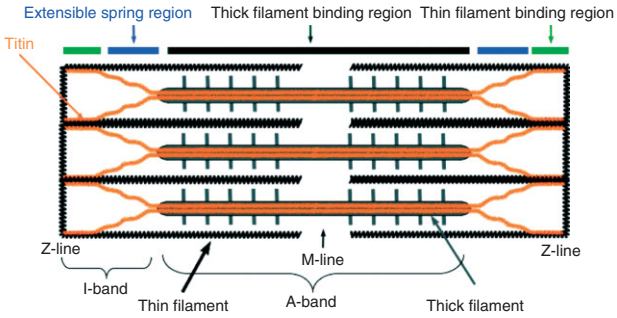

FIGURE 2 | Schematic representation of the cardiac sarcomere. The sarcomere is made up of thick (myosin) filaments (A-band) and thin (actin) filaments (I-band), which are interconnected by titin (with segments shown by colored bars on the top). The Z-line is the boundary between sarcomeres and the M-line is central portion of the A-band (Reprinted with permission from Ref 5. Copyright 2008 The Company of Biologists).

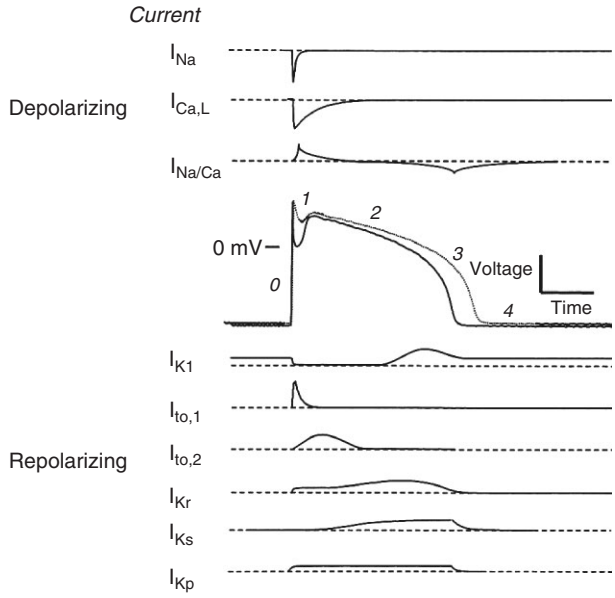

FIGURE 3 | Schematic of the membrane currents that underlie a ventricular action potential (AP) shown with a control (solid line) and failing (dotted line) AP with phases labeled. (Reprinted with permission from Ref 10. Copyright 1999 Elsevier).

The fundamental unit of contraction of the cardiac muscle fiber is the sarcomere[5] (Figure 2)—the contractile apparatus between adjacent Z-lines (or Z-disks). Figure 2 shows the region of overlap of thick (myosin) and thin (actin) filaments. Myocyte contraction is accomplished by the sliding motion of the thick and thin filaments relative to one another in this region in response to elevated levels of intracellular Ca. We will describe recent approaches to modeling of cardiac myocyte muscle contraction.

The proteins that underlie membrane currents, CICR, energy production, and contraction, are regulated via a variety of signaling pathways. The activation of signaling cascades results in posttranslational modifications of target proteins (e.g., phosphorylation of LCCs) which alter their functional properties and/or regulate protein trafficking and gene transcription, and hence, the abundance of certain functional proteins. Cell signaling pathways are complex, involving cascades of signaling molecules, multiple protein targets, and interactions among different pathways. Two of the most thoroughly studied signaling pathways in the cardiac myocyte are the β-adrenergic and Ca/calmodulin-dependent kinase II (CaMKII) pathways, and models of each have been developed. We will review models of cell signaling in the cardiac myocyte.

MODELS OF THE CARDIAC MYOCYTE ACTION POTENTIAL

Processes Underlying the Cardiac Action Potential

Figure 3 illustrates the major ionic currents giving rise to the mammalian cardiac AP.[10] Currents mediating the AP upstroke (Phase 0) are the fast inward sodium (Na) current[11] (I_{Na}), and to a lesser extent the L-type Ca current[12] (I_{CaL}). The Phase 1 notch, apparent in ventricular myocytes isolated from epi- and mid-myocardial regions but largely absent in those from the endocardium, is produced by activation of the voltage-dependent transient outward potassium (K) current[13] ($I_{to,1}$). A transient voltage-independent Ca-activated chloride current ($I_{to,2}$) may also contribute to the Phase 1 notch[14]; however, whether this current contributes to shaping the human AP remains controversial.[15] During the Phase 2 plateau, membrane conductance is very low, with the plateau potential and duration being regulated by a delicate balance between inward and outward currents. The major inward plateau current is I_{CaL}, major outward plateau currents are the rapid and slow-activating delayed rectifier currents (I_{Kr} and I_{Ks}, respectively),[16,17] and the plateau K current is I_{Kp}.[18] The initial portion of repolarization Phase 3 results from activation of I_{Kr} and I_{Ks}, and the later phase is due to the inward rectifier K current I_{K1}.[19]

At least three major ion pumps and exchangers play an important role in shaping properties of the cardiac AP, Ca transient, and in long term regulation of intracellular ion concentrations. These are the sarcolemmal Na–K pump, the Na–Ca exchanger, and the SR Ca-ATPase. The sarcolemmal Na–K pump,[20,21] present in virtually all mammalian cell membranes, hydrolyzes one ATP in order to extrude three Na

ions while importing two K ions on each cycle. The net charge movement of this electrogenic pump generates outward membrane current, which influences both AP duration (APD) and resting potential. This pump functions to keep intracellular Na low, and thereby maintains the transmembrane Na gradient by extruding Na that enters during each AP. During diastole, the sarcolemmal Na–Ca exchanger is believed to import three Na ions for every Ca ion extruded, yielding a net inward charge movement[22] (see Ref 23 for recently proposed alternative transport modes). It is the principal means by which Ca that enters the cell during the AP is extruded from the myocyte. It is driven by transmembrane voltage and intra- and extracellular Na and Ca ion concentrations. It can also function in reverse mode during the AP, in which case it extrudes Na and imports Ca, thus generating a net outward current.[24,25] The duration of reverse mode Na–Ca exchange, and hence its effect on AP shape, has been shown to vary with species, heart failure, and other factors.[26,27] The second major cytoplasmic Ca extrusion mechanism is the SR Ca-ATPase, which pumps Ca released from the JSR back into the NSR. The SR Ca-ATPase has both forward and reverse components.[28]

Early Models of the Cardiac AP

The foundation of quantitative modeling of the cardiac AP was established in the early 1960s by Denis Noble, who presented the first computational models of a cardiac myocyte—the Purkinje cell.[29,30] These models were developed to investigate the mechanisms underlying long duration APs observed in cardiac myocytes. To do this, the Hodgkin and Huxley description of the squid giant axon AP[31] was modified. The model was able to explain the long plateau phase as a balance between a maintained inward Na current and a slowly activating outward K current. Either a stable resting potential or a stable oscillation could be produced by adjusting the relative Na and K conductances, thereby mimicking the long duration, slow, oscillatory APs of the cardiac Purkinje fiber. While this model provided insight into the fundamental process involved in long duration APs, it is now known that the inward current during the plateau phase is primarily due to membrane Ca permeability. These models were subsequently extended by McAllister et al.[32] However, the experimental data on which this and other models of this era were based were flawed due to an inability to establish adequate spatiotemporal voltage clamp, and to control for changes in K concentration in the extracellular clefts of multicellular preparations.[33]

The first computational model of the mammalian cardiac ventricular myocyte was developed by Beeler and Reuter in 1977.[34] The model described four distinct membrane currents: (1) the fast inward sodium current I_{Na}; (2) a slow inward current I_s carried predominantly by Ca; (3) a time-independent inward rectifier potassium current I_{K1}; and (4) a time-dependent outward K current I_{X1}. Membrane currents were modeled using the Hodgkin–Huxley formalism. Properties of the model AP were shown to agree qualitatively with those measured experimentally. The Beeler–Reuter model is significant in being the first attempt to quantify mechanisms of the ventricular cell AP. The model reinforced the concepts that the AP plateau phase is controlled by a balance between K (I_{X1}) and Ca (I_s) currents, and repolarization is controlled by inactivation of I_s coupled with slow activation of I_{X1}. The model was the first to describe the time-varying concentration of an intracellular ionic species (Ca) within its 'small distribution volume' as a dynamic state variable.

Subsequent elaboration of these and other models led to the development of the landmark DiFrancesco–Noble (DN) model of the cardiac Purkinje fiber.[35] This model was groundbreaking in that it described: (1) hyperpolarizing-activated, Na and K permeant G_f conductance that contributes to pacemaking in Purkinje fibers; (2) time-varying concentration of K in the extracellular cleft, and intracellular concentrations of Na, K, and Ca; (3) activity of the Na–K pump and Na–Ca exchanger; and (4) voltage- and Ca-dependent inactivation of the Ca current. It introduced models of the transport of Ca into the NSR by the SR Ca-ATPase, diffusion of Ca from NSR to JSR, and CICR from the JSR. This model established the conceptual framework on which all subsequent models of the myocyte have been built. Modifications of the DN model soon led to the development of SA node[36–39] and atrial cell models.[38,40]

Computational modeling of the cardiac myocyte has advanced significantly since the days of the DN model. Tables 1 and 2 are updates to a summary of existing cardiac myocyte models first presented by Wilders.[41] Models of rabbit SA node cells,[1,36,37,39,42–48] some of which describe regional variations in cell properties,[1,44–46] have been developed. Insight into the relationship between spontaneous diastolic Ca release and the AP firing rate has been gained through the use of computational modeling to better understand mechanisms of a complex integrative theory of SA node pacemaking—the 'Ca Clock Hypothesis'.[47,48] Models of both rabbit[38,40] and human[49,50] atrial cells as well as rabbit AV node cells[51] and human Purkinje fibers[52] have been

TABLE 1 | Purkinje, SA Node, Atrial, and AV Node Cell Models Based on Tables 1 and 2 of Wilders[41]

	Authors	Species
Purkinje cell models	Noble[29]	Generic
	Noble[30]	Generic
	McAllister et al.[32]	Generic
	DiFrancesco and Noble[35]	Generic
	Stewart et al.[52]	Human
Sinoatrial node cell models	Yanagihara et al.[53]	Rabbit
	Bristow and Clark[54]	Rabbit
	Irisawa and Noma[55]	Rabbit
	Noble and Noble[36]	Rabbit
	Noble et al.[37]	Rabbit
	Rasmusson et al.[56]	Bullfrog
	Wilders et al.[57]	Rabbit
	Noble et al.[39]	Rabbit
	Dokos et al.[58]	Rabbit
	Cai et al.[1]	Rabbit
	Demir et al.[42]	Rabbit
	Dokos et al.[43]	Rabbit
	Endresen et al.[59]	Rabbit
	Zhang et al.[44]	Rabbit
	Zhang et al.[45]	Rabbit
	Kurata et al.[60]	Rabbit
	Garny et al.[61]	Rabbit
	Sarai et al.[62]	Rabbit
	Lovell et al.[46]	Rabbit
	Maltsev et al.[47]	Rabbit
	Vinogradova et al.[48]	Rabbit
	Mangoni et al.[63]	Mouse
	Maltsev and Lakatta[64]	Rabbit
Atrial cell models	Hilgemann and Noble[40]	Rabbit
	Earm and Noble[38]	Rabbit
	Lindblad et al.[65]	Rabbit
	Courtemanche et al.[50]	Human
	Nygren et al.[49]	Human
	Ramirez et al.[66]	Canine
	Aslanidi et al.[67]	Rabbit
	Maleckar et al.[68]	Human
AV node cell models	Liu et al.[69]	Rabbit
	Inada et al.[51]	Rabbit

developed. Tremendous advances have been made in modeling of the cardiac ventricular myocyte (Table 2). These advances are the focus of the remainder of this review.

Modern Computational Models of the Ventricular Myocyte AP

The first ventricular cell models based on voltage-clamp recordings obtained from isolated myocytes were reported in 1991. The ability to record from isolated cells greatly enhanced spatiotemporal control of voltage clamp and also enabled control of extracellular ion concentrations. These models were the Oxsoft HEART Version 3.3 ventricular cell model by Noble et al.,[70] and the Luo–Rudy Phase I ventricular myocyte model.[71] Both models were based on experimental data from small mammalian hearts, primarily that of guinea pig.

The Noble model was derived from prior atrial cell models,[38,40] which were in turn modifications of the 1985 DN model.[35] This model was shown to approximate AP and Ca transient waveforms measured in isolated ventricular myocytes, and was also used to investigate the role of the Na–Ca exchange current in shaping AP characteristics. While this model provided significant insights into processes regulating AP shape, its impact was limited due to the lack of full publication of model equations.

In 1991, Luo and Rudy published the Luo–Rudy Phase I model of the guinea pig ventricular cell.[71] The model described six distinct membrane currents: (1) fast inward Na current I_{Na}; (2) the slow inward current I_{si} (from Beeler and Reuter[34]); (3) a time-dependent delayed rectifier K current I_K; (4) a time-independent inward rectifier current I_{K1}; (5) the plateau K current; and (6) a background K current. Intracellular Ca cycling, sarcolemmal Na–Ca exchange, Na–K pumping, and temporal variation of intracellular ion concentrations were not described in this model. The Luo–Rudy Phase I model represented a step forward in that: (1) descriptions of ionic currents were carefully based on existing experimental data; (2) model equations were fully published, enabling model implementation by other investigators; and (3) the model was able to account for a range of experimental measurements on ventricular cell responses. Its shortcomings were that it retained the original slow inward current description of the Beeler–Reuter model and did not describe any aspect of intracellular Ca cycling.

Another landmark was the formulation of the Luo–Rudy Phase II model.[73,74] The model included the following changes: (1) sarcolemmal Na–K and Ca pumps; (2) Na–Ca exchange; (3) Ca buffers; (4) a non-specific Ca-activated current; and (5) CICR and Ca cycling. Because of the extent to which formulations of membrane currents and model predictions have been validated against experimental data, and the full publication of model equations, the Luo–Rudy

TABLE 2 | Ventricular Myocyte Models Based on Tables 1 and 2 of Wilders[41]

Authors	Species	Parent Model Authors	Novel Features
Beeler and Reuter[34]	Mammal	McAllister et al.[32]	First ventricular cell model
Noble et al.[70]	Guinea pig	Earm and Noble[38]	Based on voltage-clamp recordings in isolated cells
Luo and Rudy[71]	Guinea pig	Beeler and Reuter[34]	Based on voltage-clamp recordings in isolated cells, pumps/exchangers, Ca buffers
Nordin[72]	Guinea pig	DiFrancesco and Noble[35]	Updated currents and Ca cycling, myoplasmic compartments, homeostatic system
Luo and Rudy[73,74]	Guinea pig	Luo and Rudy[71]	Updated currents based on wide array of isolated myocyte data, variable ionic concentrations
Jafri et al.[75]	Guinea pig	Luo and Rudy[73]	Dyadic subspace, mode-switching L-type Ca channel (LCC) Markov model
Noble et al.[76]	Guinea pig	Noble et al.[70]	Dyadic space, length- and tension-dependent processes
Priebe and Beuckelmann[77]	Human	Luo and Rudy[73]	First human model
Winslow et al.[78]	Canine	Jafri et al.[75]	First canine model, Ca mediated prolongation of action potential (AP) in heart failure
Pandit et al.[79]	Rat	Demir et al.[42]	First adult rat model, transmural variations
Hund et al.[80]	Guinea pig	Luo and Rudy[73]	Ionic charge conservation constraints
Puglisi and Bers[81]	Rabbit	Luo and Rudy[73]	Heart failure, user-friendly graphical interface
Bernus et al.[82]	Human	Priebe and Beuckelmann[77]	Efficient, reduced model for use in tissue simulations
Fox et al.[83]	Canine	Winslow et al.[78]	Updated K and Ca currents, show ionic bases of APD alternans
Greenstein and Winslow[84]	Canine	Winslow et al.[78]	Stochastically simulated local control of sarcoplasmic reticulum (SR) Ca release
Cabo and Boyden[85]	Canine	Luo and Rudy[73]	Remodeling in epicardial border zone of infarct, drug effects on AP
Matsuoka et al.[86]	Guinea pig		Integrated contraction and ATP-mediated effects
Iyer et al.[87]	Human	Winslow et al.[78]	Updated currents, Markov models including I_{Na}
Matsuoka et al.[88]	Guinea pig	Matsuoka et al.[86]	ATP metabolism
Bondarenko et al.[89]	Mouse		Markov models, apex/septum variations
Shannon et al.[90]	Rabbit	Puglisi and Bers[81]	Luminal SR Ca-dependent RyR, submembrane Ca space
ten Tusscher et al.[91]	Human		Updated currents, transmural variations
Hund and Rudy[92]	Canine	Luo and Rudy[73]	CaMKII regulation, chloride handling
Greenstein et al.[93]	Canine	Greenstein and Winslow[84]	Simplified local control of SR Ca release
Cortassa et al.[94]	Guinea pig	Winslow et al.[78]	Integrated mitochondrial bioenergetics and contraction
Crampin and Smith[95]	Guinea pig	Luo and Rudy[73]	EC coupling with pH regulation
Crampin et al.[96]	Rat	Pandit et al.[79]	EC coupling with pH regulation
Mahajan et al.[97]	Rabbit	Shannon et al.[90]	Markovian LCC, fast rate Ca alternans
Pasek et al.[98]	Guinea pig	Nordin,[72] Noble et al.,[76] and Faber and Rudy[99]	Diffusive transverse-axial tubule system, heterogeneous ion channel distribution
Wang and Sobie[100]	Neonatal mouse	Bondarenko et al.[89]	Neonatal currents and Ca cycling
Hashambhoy et al.[101]	Canine	Greenstein and Winslow[84]	CaMKII regulation, LCC phosphorylation (I_{CaL} facilitation)
Korhonen et al.[102]	Mouse embryonic cardiomyocyte		E9–E11 myocytes, Ca oscillations underlying pacemaking and EC coupling
Korhonen et al.[103]	Neonatal rat		Radial Ca diffusion between sarcolemma, SR, and nucleus
Grandi et al.[104]	Human	Shannon et al.[90]	Updated K currents and Ca handling, Na accumulation
Koivumaki et al.[105]	Mouse	Bondarenko et al.[89]	CaMKII regulation of EC coupling

Phase II model and its subsequent enhancements have become the most extensively used cardiac ventricular cell models.

Publication of the Luo–Rudy Phase II model marked the beginning of an era in which computational models of the cardiac ventricular myocyte have become increasingly biophysically detailed. Development of new experimental techniques has provided extensive data describing the functional components within the cardiac myocyte. Many advances in integrative modeling of the ventricular myocyte have resulted from quantitative modeling of these components and their addition to existing models. This has sometimes required the solution of thousands of differential equations or the stochastic simulation of up to $\sim 10^6$ single channels in a single cell. These computations are now tractable. Some important advances in modeling of the ventricular myocyte are described in the following section. In this short review, we cannot possibly do justice to all the important work that has brought us to where we are today. We have therefore chosen to focus on development of major new functional components, their integration into whole cell models, and the insights that have been obtained from these advances in modeling capabilities.

MODELING FUNCTIONAL COMPONENTS OF THE CARDIAC VENTRICULAR MYOCYTE

Modeling Voltage-Gated Ionic Currents

For many years, Hodgkin–Huxley models have been the standard for describing voltage-dependent membrane ion current dynamics.[31] These models introduced the concept of activation and inactivation gates, and related the current through an ensemble of channels to the state of these gates. The brilliance of Hodgkin and Huxley is that they developed experimental techniques for measuring properties of activation and inactivation using the voltage-clamp recording technique.

More recent data obtained using new experimental approaches for measuring single-channel openings and closings have shown that Hodgkin–Huxley models have significant limitations, often due to the assumption that channel gates behave independently. This assumption can be relaxed by using continuous-time Markov chain models[106] to describe channel gating and ionic currents. Markov chain models are comprised of a number of different states, loosely corresponding to different conformations of channel protein(s) as they undergo activation and inactivation, with transition rates between certain states being

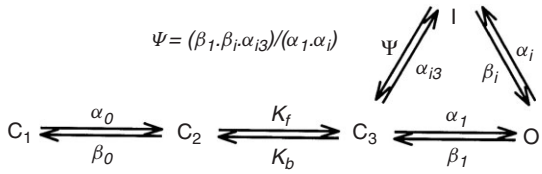

FIGURE 4 | State diagram of the HERG and HERG+hKCNE2 Markov model. C_I, C_2, and C_3 are closed states, O is the open state, and I is the inactivated state (Reprinted with permission from Ref 110. Copyright 2001 American Heart Association).

voltage-dependent. While a Hodgkin–Huxley model can be expanded to an equivalent Markov chain representation,[107] often many single-channel behaviors such as mean open time, first latency, and a broad range of other kinetics behaviors are not well described using this equivalent model.[108,109]

An example of a Markov chain model of the HERG and HERG+hKCNE2 channel is shown in Figure 4. This model was used by Mazhari et al.[110] to interpret their experimental data regarding the functional role of co-expression of hKCNE2 with HERG (the two molecular components of I_{Kr}). Markov models are parameterized by the state transition rates. These rates reflect the free energy profile between two protein conformations[107] and must be determined experimentally. This is done through application of various voltage-clamp protocols, recording current responses, and adjusting the transition rates using minimization algorithms to yield a best fit to the data. In some instances, single-channel patch-clamp recordings have been used to constrain Markov models. Markov models of ion currents are now used extensively. Applications have included quantitative modeling of the effects of channel mutation,[111–114] drug–channel interactions,[115–118] channel phosphorylation,[101,119] and channel-subunit interactions[110] on myocyte responses. These whole cell models have been shown to have predictive value.

Now there are many Markov membrane current models that, for each current, can differ radically in their number of states and interconnection topology (e.g., I_{Na},[114,119,120] I_{Kr},[110,113,121,122] and I_{CaL}[75,97,123]). If several channels in a single cell model are modeled using the Markov formulation, the aggregate number of state equations may become large. Consequently, use of Markov models imposes increased computational load. However, the advent of faster, multicore processors and graphics processing units is making this less of a problem at both the cellular and tissue levels. In addition, use of complex state models at the cellular level does not impose a major additional computational load when simulating these models stochastically because the Markov property assures that the future evolution of the

process state depends only on the nature of the current state and not on the number of states in the model.

Modeling Sarcolemmal Membrane Transporters

The first myocyte model to explicitly describe membrane transporter function was the DN model.[35] The Na–K pump, Na–Ca exchanger, and the SR Ca-ATPase were modeled as algebraic functions of the relevant intracellular and extracellular Na, Ca, and K concentrations. These models were refined and constrained using experimental data in the work of Luo and Rudy.[73] In 1998, Shannon et al.[124] proposed a new model of the SR Ca-ATPase that included forward- and reverse-current components, each with its own Ca-binding constant and peak forward and reverse rates. This model is now used extensively, and has been integrated into the models of Winslow et al.,[78] Puglisi and Bers,[81] Shannon et al.,[90] and Grandi et al.[104] Recently, carefully constrained Markovian models of the Na–K pump,[125] the SR Ca-ATPase,[126] and Na–Ca exchanger[23] have been published but have not yet been incorporated in whole cell models. The first model of intracellular pH regulation, based on phenomenological representations of transmembrane acid fluxes in guinea pig, was developed by Leem et al.[127] More recently, Crampin et al.[96] and Crampin and Smith[95] have developed models of the sarcolemmal: (1) Na–H ion exchanger; (2) Na–HCO_3 cotransporter; (3) Cl/OH exchanger; and (4) the anion exchanger. Models of pH regulation have been incorporated into the Luo–Rudy model and used to study the effects of acidosis in ischemia on excitation–contraction (EC) coupling. Results predict that changes in cytosolic Ca transients in acidosis are primarily due to direct inhibition of the Na–Ca exchanger and a rise in intracellular Na levels.

Modeling Intracellular Calcium Cycling and Calcium-Induced Calcium-Release

At rest, low levels of Ca in the dyad lead to a low RyR open probability. During the initial stages of the AP, voltage-gated LCCs in the sarcolemmal membrane open and Ca ('trigger Ca') enters the dyadic space. This Ca binds to RyRs, increasing their open probability and producing CICR. The amount of Ca released from the JSR is significantly greater than the amount of trigger Ca.[128] The ratio of Ca released from JSR to the amount of trigger Ca entering the myocyte is referred to as the EC coupling gain. Graded release refers to the phenomenon, originally observed by Fabiato et al.,[129] that Ca release from JSR is graded according to the amount of trigger Ca entering the cell via LCCs.

Many advances in cardiac myocyte models over the past decade have resulted from improved descriptions of the underlying mechanisms of CICR. In 1998, Jafri et al.[75] presented a model of the guinea pig ventricular myocyte whose membrane currents were largely based on those of the Luo–Rudy Phase II model. This model was the first to incorporate mechanistic Markov models for both LCCs and RyRs, and was also the first to implement a 'restricted subspace', a single compartment representing the total volume of all dyads into which all Ca fluxes through RyRs and LCCs are directed. The major prediction of this model was that experimentally measured interval-force (transient) and frequency-force (steady-state) relationships could be explained by the interplay between RyR inactivation and SR Ca load dynamics. Shortly thereafter, this Ca subsystem was modified for canine in the model of Winslow et al.[78] The model predicted that negative feedback produced by Ca release from the JSR and the subsequent Ca-dependent inactivation of LCCs was a powerful factor regulating APD. This prediction was subsequently validated by studies of Alseikhan et al.[130] in which APD was shown to be dramatically prolonged by knockout of Ca binding to calmodulin and the resulting ablation of Ca-dependent inactivation of LCCs.

While the models described above successfully predict mechanisms underlying experimentally observed Ca transients and APs in both normal and diseased cells, they cannot reproduce graded SR Ca release because they are 'common pool' models. As defined by Stern[131] in 1992, common pool models are those in which LCC trigger Ca enters the same cytosolic Ca pool into which SR Ca is released. The rapid increase of Ca in this pool in turn leads to non-physiological regenerative, all-or-none rather than graded Ca release. Stern elegantly demonstrated that common pool models cannot achieve both high gain and graded Ca release.[131]

One way to circumvent this problem is to model SR Ca release flux as a phenomenological function of LCC influx and/or membrane potential.[74,83,89,91,92,97] Doing so removes the positive feedback effect inherent to common pool models. Models incorporating this phenomenological mechanism have been successful in describing many myocyte behaviors. However, as with any phenomenological approach, the predictive power of such models must always be questioned. By formulating a model in which it was assumed that a single LCC can trigger SR Ca release only from a locally apposed cluster of RyRs, Stern demonstrated that graded release arises as the result of statistical recruitment of release clusters.[132] This process is known as local control of Ca release. Discrete

Ca release events can now be measured experimentally, and are known as Ca sparks.[133] The first comprehensive model of the myocyte based on the theory of local control was developed by Greenstein and Winslow.[84] This model includes a population of dyadic Ca release units in which local interactions of individual sarcolemmal LCCs and nearby RyRs are simulated stochastically. This multiscale approach to model construction resulted in the ability to reproduce experimentally observed behaviors on both microscopic (single-channel gating and discrete Ca release events) and macroscopic scales (graded SR Ca release, voltage-dependent EC coupling gain, whole cell Ca transients, and APs). Application of the model demonstrated that local control is an essential property for stability of APs when the LCC inactivation process depends more strongly on local Ca than on membrane potential. Subsequently, a simplified local control model of CICR[134–136] was formulated by applying a carefully chosen set of approximations that allow for the ensemble behavior of Ca release units to be represented by a low dimensional system of ordinary differential equations. Incorporation of this coupled LCC–RyR model into that of Greenstein and Winslow[84] yielded the ventricular myocyte model of Greenstein et al.[93] which could reproduce all the core features of its predecessor, but without the computationally expensive stochastic simulations, making it a candidate for use in large-scale tissue simulations.[137] This model was able to predict aspects of the underlying relationship between macroscopic EC coupling gain and single-channel properties of LCCs measured experimentally.[138]

The rabbit ventricular myocyte model of Shannon et al.[90] was the first to introduce a subsarcolemmal Ca compartment, based on experiments that suggested Ca-dependent transport mechanisms are sensing elevated Ca levels.[26,139] Another novel feature of the Shannon et al.[90] rabbit model was the formulation of an RyR model with dynamics that depend on both cytosolic and SR luminal Ca levels. This model was modified from that of Stern et al.[140] so that Ca binding to the luminal site increased the affinity of the cytosolic activation site, while decreasing the affinity of the cytosolic inactivation site for Ca. This novel regulatory feature underlies the ability of the Shannon et al.[90] model to reproduce experimentally characterized relationships between SR Ca load and properties of SR Ca release,[141,142] and assigns an important role to the (partial) depletion of luminal JSR Ca level in the dynamic regulation and termination of SR Ca release. Using this model, Shannon et al.[143] demonstrated that the role of RyR regulation by luminal Ca may be to adjust steady-state SR Ca level in response to alteration in RyR Ca sensitivity, as originally proposed by Eisner et al.[142] Despite the success of this model, its reliance in part on cytosolic Ca-dependent inactivation for termination of SR Ca release conflicts with recent experiments,[144–146] and the underlying mechanisms of SR release termination remain controversial and not well understood.

Modeling Metabolism

The first computational models of metabolic dynamics of substrate utilization and energy transfer in cardiac myocytes were formulated in the late 1970s by Garfinkel and coworkers.[147,148] These pioneering comprehensive models, encompassing about 90 biochemical reactions, were formulated with individual biochemical reactions described by either mass action laws or Michaelis–Menten kinetics.[149,150] Several pathways, such as glycolysis, β-oxidation, and oxidative phosphorylation, were included in these early formulations. The models also accounted for compartmentalization, transport of intermediary metabolites between compartments, and regulatory interactions such as the effect of ATP and ADP on the activity of glycolytic enzymes.[148,151,152] Model simulations supported the idea that adenine nucleotides were key regulators of cellular energy production,[153] in agreement with studies of isolated mitochondria,[154] which described how 'respiratory control' of energy metabolism is coupled to cellular energy demand through the effects of adenine nucleotide phosphorylation potential on mitochondrial oxygen consumption.

However, subsequent results obtained with ^{31}P NMR showed that bulk ATP and phosphocreatine levels were relatively insensitive to changing workload conditions in the short term, challenging the 'respiratory control' mechanism for matching energy supply with demand.[155] As an alternative, Saks and coworkers hypothesized that energy transfer dynamics occurred at the sites of energy production and consumption, introducing the concept of 'intracellular energetic units'.[156] A model accounting for generation of gradients of ADP around myofibrils, where active ATP consumption occurs during contractile activity, was postulated.[157] The linear dependence of the respiratory rate with workload, as measured through changes in cardiac volume in the Frank–Starling mechanism, could be quantitatively explained with such a model of reaction–diffusion of adenine nucleotides and creatine metabolites. This model further assumed that the creatine kinase reaction is operating far from equilibrium at the sites of energy consumption and in the mitochondrial intermembrane space.[158] The subsequent work of van Beek[159] challenged this notion

and concluded that a combination of cytoplasmic phosphate buffering reactions (creatine kinase and glycolysis) predominates to influence the adaptation rate. A model of ADP diffusion and interconversion of ADP/ATP with creatine could reproduce the fast response.[160,161]

Ischemia–reperfusion represent a major challenge for computational modeling of myocardial metabolism. Initial work was done by Ch'en et al.[162] They developed a model describing proton transport across the sarcolemmal membrane, and lumped biochemical reactions accounting for glycogen degradation into lactate, creatine kinase equilibrium, and ATP hydrolysis, including pH-associated changes. Simulations of contractile failure and contracture after 5 min of total ischemia reproduced experimental data on the consumption of internal glycogen stores and the exhaustion of creatine phosphate followed by ATP depletion.[162] However, most mathematical expressions used in this model were phenomenological rather than mechanistic. Further model development has focused on a more detailed representation of pH regulation and generation of pH gradients, and oxidative phosphorylation in cardiomyocytes.[163,164]

In 2003, Cortassa et al.[165] formulated a mechanistic model of mitochondrial energy production that included Ca transport, regulation of tricarboxylic acid cycle dehydrogenases by calcium, and the electrochemical driving forces that describe the fundamental relationship between mitochondrial membrane potential and respiratory rate, as observed in isolated mitochondria treated with oligomycin and rotenone and titrated with the uncoupler FCCP (carbonyl cyanide p-trifluoromethoxyphenylhydrazone).[166] By simulating extra-mitochondrial Ca pulses, this model could also reproduce the temporal profile of NADH changes associated with alterations in pacing frequency in intact cardiac muscle.[167] Using a similar approach, Nguyen and Jafri[168] modified the Ca transport rate equations and added phosphate transport. The resulting model simulates a linear relationship between mitochondrial Ca and cytoplasmic Ca that the authors used to reproduce experimental data from the Lemasters group.[169] Beard and coworkers developed a model of mitochondrial function including linear force–flow relations between respiration and its driving forces, and potassium and phosphate ion dynamics. The model is able to simulate respiratory rates and NADH levels that are observed with isolated mitochondria in the presence of different levels of inorganic phosphate.[170,171]

Integrating mitochondrial energetics into models of cardiomyocyte function is the natural step forward to understand heart physiology and pathophysiology. Simulations of NADH and mitochondrial Ca transients, following an increase in workload, were achieved by changing the stimulation frequency by the 'Kyoto' model in which Korzeniewski's mitochondrial metabolic model was coupled to the electrophysiological model of Noma.[88] Model simulations were able to show that ~23% of the increase in the rate of ATP synthesis in response to an increase in workload was met by Ca activation of dehydrogenases, whereas the remaining 77% was assigned to 'respiratory control'.[172] The excitation–contraction coupling and mitochondrial energetic (ECME) model[94] (Figure 5) was built by integrating the mitochondrial energetics[165] and EC coupling models, the latter describing the dynamics of electrophysiological and contractile processes in the guinea pig.[173] The ECME substantiates the participation of mitochondria in Ca buffering,[174] which is transported across the inner mitochondrial membrane through the Ca uniporter and the mitochondrial Na–Ca exchanger. One of the main contributions of the ECME model has been to clarify the role of ADP and Ca as two main signaling mechanisms participating in matching energy supply with demand at different workloads in heart trabeculae.[167,175] Further studies of metabolic control performed with the ECME model at rest or working conditions revealed the importance of the myofibrilar ATPase activity as a rate-controlling step of mitochondrial respiration; the regulatory function of adenine nucleotides in the response of bioenergetic processes could also be demonstrated in the context of integrated cardiomyocyte function.[176] Extensions of the ECME model have been used to investigate mechanisms of oxidative stress.[177–181]

Modeling Excitation–Contraction Coupling

The heart cell can be considered a coupled electromechanical system in which the AP triggers an increase in intracellular Ca and contraction of the myofilaments that allows the heart to pump. Troponin is the largest buffer of Ca in the cell, and affinity of the Ca-binding regulatory sites on troponin is thought to be a function of force generated by the myofilaments. The Ca transient is in fact altered when developed force is changed.[182] Therefore, including myofilament binding of Ca is not only crucial for modeling force generation by the myocyte, but is also important for realistic modeling of cytosolic Ca transients and Ca cycling. Here, we provide an overview of myofilament modeling. More complete descriptions may be found elsewhere.[183,184]

In cardiac muscle, each troponin molecule can bind Ca at two high-affinity and one low-affinity binding sites. The lower affinity site serves

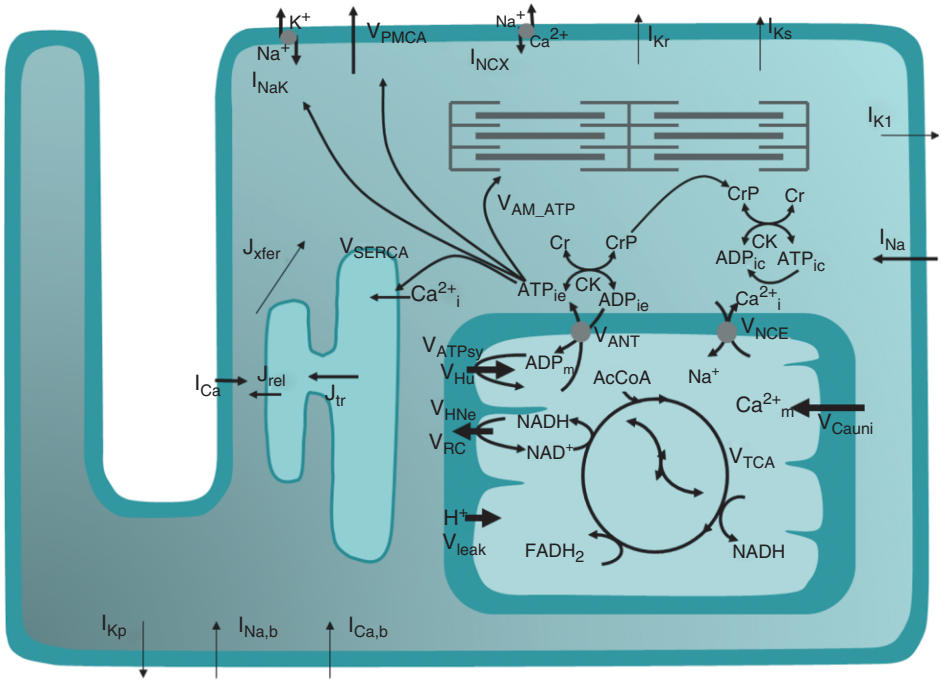

FIGURE 5 | General scheme of the excitation–contraction coupling-mitochondrial energetics guinea pig model including membrane currents, sarcolemmal ion transport, Ca compartmentalization, and mitochondrial function.

a regulatory function because, in the steric hindrance model, Ca binding produces an allosteric shift of troponin/tropomyosin on the thin filament to allow actin–myosin interactions. Troponin/tropomyosin units connect end-to-end and form two-strand helices that wrap around the thin filaments in the myofilaments of the myofibrils. Myosin protrudes from the thick filaments, and when allowed, forms crossbridges with the actin in the thin filament. While the steric hindrance model is generally accepted, the detailed mechanisms remain controversial.[23,185]

Many different myofilaments models are being developed by numerous groups.[88,186–193] The diversity reflects both the lack of consensus regarding the appropriate mathematical formalisms needed to describe the biophysics, as well as controversies regarding which mechanisms are most salient to muscle responses.[183] Here, we review a subset of force generation models that describe both the cardiac AP and function of the myofilaments in order to illustrate the progression of the field:

The Hilgemann–Noble (HN) model[40] of rabbit atrium incorporated one ordinary differential equation to represent Ca-based activation, and a second to represent crossbridge binding. This formulation was presented as an abstract description of force generation, and some aspects of the model are now known to be inconsistent with current data. For example, in the HN model, binding of Ca to both high- and low-affinity sites affects activation, whereas it is now known that only low-affinity sites are regulatory in cardiac muscle. By assuming multiple binding sites, the HN model exhibited an increased Ca sensitivity and Hill coefficient similar to cardiac muscle. This basic formulation was carried on to models later developed by Noble and coworkers,[38] including model extensions for describing SL sensitivity.[76]

The Hunter–McCulloch–ter Keurs (HMT)[186] model couples a mechanistic myofilament activation model to a fading memory crossbridge model that uses a convolution integral approach. The model includes active force with SL dependence and passive tissue properties. Simulated responses have been compared with a wide range of experimental measures. The HMT model has been refined[194] and extended[195] recently by incorporation within a model of the rat myocyte AP formulated by Pandit et al.[79] The combined model has been used to investigate the putative mechanisms of the slow force response, a secondary prolonged increase in force beyond the Frank–Starling response. The combined model has also been used as the basis of a multiscale electromechanical model of the rat left ventricle[196] that has been used to investigate how cellular-level behaviors affect work transduction, stress and strain homogeneity at the whole ventricle level.

The Rice-Jafri-Winslow (RJW) model integrated the myofilament model of Rice et al.[188] into the model

of the guinea pig AP formulated by Jafri et al.[75] This model reproduced experimentally measured properties of mechanical restitution and post-extrasystolic potentiation. These phenomena are examples of interval–force relations in which changing the temporal spacing between APs can produce dramatic changes in developed force.[184] An important finding from this work was that altering the pacing protocol affected the amplitude of the Ca transient and force generation to a relatively small degree, while the cooperative properties of the myofilaments produced a much larger relative change in developed force. The model included a phenomenological representation of cooperative interactions between neighboring troponin/tropomyosin units, including effects of SL. However, the RJW model was limited since only isometric force protocols could be simulated.

The RJW model has been refined and expanded to reproduce a wider variety of experimental protocols in the Rice et al. model.[182] Importantly, active contraction and re-lengthening can be simulated, and passive muscle properties are included to simulate muscle strips and isolated myocytes, two common experimental preparations. The model includes phenomenological representations of cooperative interactions between neighboring troponin/tropomyosin units and cycling crossbridges that are computationally efficient. While phenomenological approximations are employed, the overall model structure attempts to map well to the underlying biophysics. Thus, parameter definitions are intuitive and easily modified, as compared to highly lumped or abstracted parameters in fully phenomenological models. The model has been extended recently by Campbell et al.[197] to replicate canine epicardial, endocardial, and mid-myocardial myofilament responses. These cell models have been composed into a tissue model to investigate the heterogeneous layers in the ventricles.[198] Tran et al.[199] have modified the Rice et al. model to include binding and release of metabolites: ATP, ADP, Pi, and H.

Modeling Regulation via Cell Signaling

Cardiac ion channels as well as proteins involved in CICR and EC coupling are primary targets for regulation via cell signaling pathways. The most widely studied pathway is that of the β-adrenergic signaling cascade (Figure 6). The 'fight or flight' response increases cardiac contractility and output via the release of neurotransmitters and hormones by the sympathetic nervous system. Norepinephrine and epinephrine bind to β-adrenergic receptors (β-ARs) on the myocyte surface. These are G-protein-coupled receptors which trigger the activation of adenylyl cyclase (AC), leading to the production of cyclic AMP (cAMP), which in turn activates protein kinase A (PKA). The numerous targets of PKA-mediated phosphorylation include LCCs, RyRs, phospholamban (PLB, a regulator of the SR Ca-ATPase), the myofilament protein troponin I, and phospholemmen (a subunit of the Na–K pump).[3,200,201] Early attempts to model the effects of PKA-mediated phosphorylation of these targets on the properties of CICR and the AP involved modeling the stimulated cell by altering the function of the target proteins based on

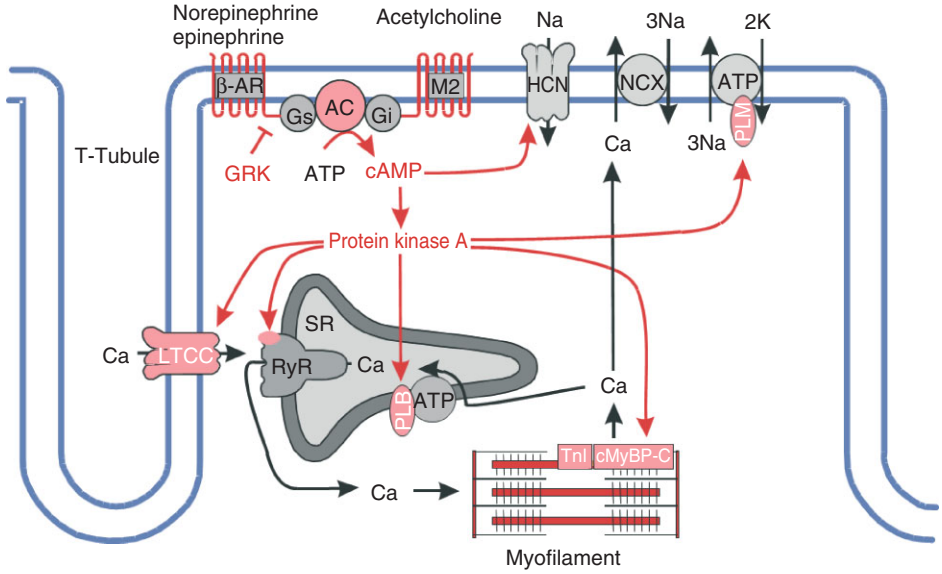

FIGURE 6 | Protein kinase A signaling pathways in cardiac myocytes (Reprinted with permission from Ref 200. Copyright 2008 Springer Science+Business Media). See text and Figure 2 of Ref 200 for further details.

the measured effects of phosphorylation. Greenstein et al.[202] developed a model of the canine ventricular myocyte in the presence of 1 μM isoproterenol (a β-AR agonist). This model could explain PKA-mediated changes in AP shape, dissected the specific effects of PKA-mediated phosphorylation of LCCs and RyRs on the voltage-dependent gain of CICR, and predicted a mechanism by which increasing levels of LCC phosphorylation could lead to increased frequency of early afterdepolarizations.[203] However, this model did not describe the dynamics of the β-adrenergic signaling pathway. Saucerman et al.[204] developed a differential-algebraic model of the dynamics of the β-adrenergic signaling pathway, and incorporated it into the rabbit myocyte model of Puglisi and Bers.[81] This model was used to understand and predict effects of specific molecular perturbations (e.g., expression changes in AC and β-AR density) on cAMP dynamics and contractility via changes in function of target proteins resulting from altered phosphorylation dynamics. Recently, the model of Saucerman et al.[204] was incorporated into the guinea pig ventricular model of Faber and Rudy[99] in a study of the role of β-adrenergic agonists and antagonists in long-QT syndrome.[205]

An important Ca cycling regulatory mechanism of recent interest is the signaling pathway involving CaMKII, whose target proteins include LCCs, RyRs, PLB, and the SR Ca-ATPase, as well as Na and K channels.[206] Evidence suggests that CaMKII is directly associated with its target proteins[207,208] and that CaMKII activity is elevated in heart failure.[209] CaMKII becomes activated when its autoregulatory domain is bound by Ca-bound calmodulin (CaM), thereby exposing its catalytic domain. In addition, the phosphorylation of a CaMKII monomer by a neighboring monomer (within the dodecameric enzyme) renders the molecule 'autonomous'', where its kinase activity no longer depends on Ca binding,[210] therefore the net activity of CaMKII has a complex dependence on Ca dynamics in the local vicinity of its target proteins.

The first model of the cardiac myocyte to integrate the role of CaMKII was presented by Hund and Rudy.[92] In this model, CaMKII transitions from an inactive to an active state in response to elevated subspace Ca levels, and may also enter the trapped state in which it remains active for some time following the decline of subspace Ca. CaMKII activity is assumed to modify the function of LCCs, RyRs, PLB, and the SR Ca-ATPase. The model predicted that CaMKII plays an important role in the rate-dependent increase of the cytosolic Ca transient, but does not play a significant role in rate-dependent changes of APD. Grandi et al.[119] developed a model of CaMKII overexpression in the rabbit ventricular myocyte, including the role of CaMKII phosphorylation of fast Na channels, LCCs, and $I_{to,1}$. The CaMKII-dependent alteration of I_{Na} enhanced/stabilized its inactivation, but at the same time increased the late, non-inactivating component of current, revealing an important mechanism by which I_{Na} may modulate different properties of the AP at different pacing rates (APD at slow rates and upstroke velocity at fast rates). Combining CaMKII's effect on I_{Na} with that on I_{CaL} and $I_{to,1}$ revealed a net effect of APD reduction with CaMKII, as measured in experiments.[211] Saucerman and Bers[212] incorporated models of CaM, CaMKII, and calcineurin (CaN) into the Shannon et al.[90] model in order to better understand the functional consequences of the different affinities of CaM for CaMKII and CaN during APs. The model predicted that in the cardiac dyad, Ca levels lead to a high degree of CaM activity which results in frequency-dependent CaMKII activation and constitutive CaN activation, whereas the lower Ca levels in the cytosol only minimally activate CaM, which allows for gradual CaN activation, but no significant activation of CaMKII. Recently, Hashambhoy et al.[101] described dynamic CaMKII phosphorylation of LCCs in the context of the stochastic, local control canine ventricular myocyte model of Greenstein and Winslow.[84] In this model it is assumed that a single CaMKII holoenzyme is tethered to each LCC, and each CaMKII monomer can transition among a variety of activity states (see Figure 2 of Hashambhoy et al.[101]), and CaMKII monomers can catalyze the phosphorylation of individual LCCs. This model demonstrated that CaMKII-dependent shifts of LCC gating patterns into high-activity gating modes may be the underlying mechanism of a variety of experimentally observed phenomena associated with I_{CaL} facilitation. Hashambhoy et al.[213] further expanded this model to include CaMKII-dependent regulation of RyRs and demonstrated that under physiological conditions, CaMKII phosphorylation of LCCs ultimately has a greater effect on RyR (leak) flux and APD than phosphorylation of RyRs.

CONCLUSION

Integrative modeling of the cardiac myocyte is advancing rapidly into exciting new areas. The ever accelerating pace of model development can be attributed, in part, to the availability of published model source codes in their original electronic form. These are often made available on the World Wide Web either directly by the model authors or via a model repository such as CellML (models.cellml.com). Here, we note some important new directions for future research.

Recently, Silva et al.[214] constructed an atomic-level model of the I_{Ks} alpha-subunit KCNQ1, and used results from molecular dynamics simulations to constrain a Markov model of the I_{Ks} current, including KCNE1 β-subunit interactions. This line of work holds great promise for developing 'first principles' Markov models of channel gating and for predicting effects of channel point mutations on gating behavior.

Myocyte modeling has proceeded in a 'top down' fashion. The first step was to understand the voltage-gated membrane currents and transporters that shape the cardiac AP. Modeling of these currents has now reached an advanced level. Consequently, a new direction of research is to characterize and model the intracellular signaling pathways that modulate these primary effectors of the cardiac AP. Development of such models will be challenging, since both the dynamics of the signaling pathway itself and the actions of key signaling proteins on their molecular targets must be modeled. Models of the β-adrenergic and CaMKII signaling pathways are now under development. Other key pathways, such as the nitric oxide signaling pathway, remain to be developed.

Ca cycling and release plays a key role in both EC coupling and regulation of characteristics of the cardiac AP. In particular, the cardiac ryanodine receptor is a complex channel whose function is modulated in many different ways, including by phosphorylation, interactions with accessory subunits, potentially interactions with adjacent RyRs, JSR Ca, and a wide variety of point mutations. Altered function of RyRs is associated with increased JSR Ca leak in heart failure[214–216] and arrhythmic activity in diseases such as catecholaminergic polymorphic ventricular tachycardia and arrhythmogenic right ventricular cardiomyopathy type 2.[217] However, it has been notoriously difficult to characterize and model the behavior of these channels.

Incorporation of models of mitochondrial energetics into whole myocyte models has shed new light on the mechanisms involved in matching energy supply and demand in the heart. Looking forward, there are several important areas of further metabolic model development. The addition of computational descriptions to describe switching between different substrates, for example, due to the transcriptional activation of enzymes responsible for fatty acid metabolism, which occurs in association with cardiac disease, will be important. More refined models of the properties of Krebs cycle enzymes and the mitochondrial respiratory chain complexes will also be required in order to understand how newly discovered posttranslational modifications might impact energy flux. Another important area will be to model the interactions between metabolism and intracellular redox regulation, including effects on antioxidant pathways. Finally, models to take into account spatial considerations and information transfer between organelles (e.g., mitochondria–SR; mitochondria–nucleus) are needed for a better understanding of whole cell systems' interactions.

Development of these models will be a key step forward in integrative modeling of the myocyte.

ACKNOWLEDGEMENT

This work was supported by National Institute of Health Grants R33HL87345 and PO1HL081427.

REFERENCES

1. Cai D, Winslow RL, Noble D. Effects of gap junction conductance on dynamics of sinoatrial node cells: two-cell and large-scale network models. *IEEE Trans Biomed Eng* 1994, 41:217–231.
2. Soeller C, Cannell MB. Examination of the transverse tubular system in living cardiac rat myocytes by 2-photon microscopy and digital image-processing techniques. *Circ Res* 1999, 84:266–275.
3. Bers DM. Cardiac excitation–contraction coupling. *Nature* 2002, 415:198–205.
4. Forbes MS, Sperelakis N. Association between mitochondria and gap junctions in mammalian myocardial cells. *Tissue Cell* 1982, 14:25–37.
5. Shiels HA, White E. The Frank-Starling mechanism in vertebrate cardiac myocytes. *J Exp Biol* 2008, 211:2005–2013.
6. Balaban RS. Domestication of the cardiac mitochondrion for energy conversion. *J Mol Cell Cardiol* 2009, 46:832–841.
7. O'Rourke B, Cortassa S, Aon MA. Mitochondrial ion channels: gatekeepers of life and death. *Physiology (Bethesda)* 2005, 20:303–315.
8. O'Rourke B. Mitochondrial ion channels. *Annu Rev Physiol* 2007, 69:19–49.
9. Maack C, O'Rourke B. Excitation–contraction coupling and mitochondrial energetics. *Basic Res Cardiol* 2007, 102:369–392.

10. Tomaselli GF, Marban E. Electrophysiological remodeling in hypertrophy and heart failure. *Cardiovasc Res* 1999, 42:270–283.
11. Marban E, Yamagishi T, Tomaselli GF. Structure and function of voltage-gated sodium channels. *J Physiol (Lond)* 1998, 508:647–657.
12. Kamp TJ, Hell JW. Regulation of cardiac L-type calcium channels by protein kinase A and protein kinase C. *Circ Res* 2000, 87:1095–1102.
13. Sah R, Ramirez RJ, Oudit GY, Gidrewicz D, Trivieri MG, Zobel C, Backx PH. Regulation of cardiac excitation–contraction coupling by action potential repolarization: role of the transient outward potassium current (I(to)). *J Physiol* 2003, 546:5–18.
14. O'Rourke B, Kaab S, Tunin R, Kass DA, Tomaselli GF, Marban E. Calcium-release activated chloride currents shape the action potential in canine ventricular myocytes. *Circulation* 1996, 94:I–715.
15. Hume JR, Duan D, Collier ML, Yamazaki J, Horowitz B. Anion transport in heart. *Physiol Rev* 2000, 80:31–81.
16. Horie M, Hayashi S, Kawai C. Two types of delayed rectifying K+ channels in atrial cells of guinea pig heart. *Jpn J Physiol* 1990, 40:479–490.
17. Sanguinetti MC, Jurkiewicz NK. Two components of cardiac delayed rectifier K+ current. Differential sensitivity to block by class III antiarrhythmic agents. *J Gen Physiol* 1990, 96:195–215.
18. Yue DT, Marban E. A novel cardiac potassium channel that is active and conductive at depolarized potentials. *Pflugers Arch* 1988, 413:127–133.
19. Sakmann B, Trube G. Conductance properties of single inwardly rectifying potassium channels in ventricular cells from guinea-pig heart. *J Physiol* 1984, 347:641–657.
20. Glitsch HG. Electrophysiology of the sodium-potassium-ATPase in cardiac cells. *Physiol Rev* 2001, 81:1791–1826.
21. Therien AG, Blostein R. Mechanisms of sodium pump regulation. *Am J Physiol Cell Physiol* 2000, 279:C541–C566.
22. Reeves JP, Hale CC. The stoichiometry of the cardiac sodium-calcium exchange system. *J Biol Chem* 1984, 259:7733–7739.
23. Kang TM, Hilgemann DW. Multiple transport modes of the cardiac Na+/Ca2+ exchanger. *Nature* 2004, 427:544–548.
24. Philipson KD, Nicoll DA. Sodium-calcium exchange: a molecular perspective. *Annu Rev Physiol* 2000, 62:111–133.
25. Bers DM, Weber CR. Na/Ca exchange function in intact ventricular myocytes. *Ann N Y Acad Sci* 2002, 976:500–512.
26. Weber CR, Piacentino V, 3rd. Ginsburg KS, Houser SR, Bers DM. Na(+)–Ca(2+) exchange current and submembrane [Ca(2+)] during the cardiac action potential. *Circ Res* 2002, 90:182–189.
27. Hobai IA, O'Rourke B. Enhanced Ca(2+)-activated Na(+)–Ca(2+) exchange activity in canine pacing-induced heart failure. *Circ Res* 2000, 87:690–698.
28. Shannon TR, Ginsberg KS, Bers DM. SR Ca uptake rate in permeabilized ventricular myocytes is limited by reverse rate of the SR Ca pump. *Biophys J* 1997, 72:A167.
29. Noble D. Cardiac action and pacemaker potentials based on the Hodgkin-Huxley equations. *Nature* 1960, 188:495–497.
30. Noble D. A modification of the Hodgkin–Huxley equations applicable to Purkinje fibre action and pacemaker potentials. *J Physiol* 1962, 160:317–352.
31. Hodgkin AL, Huxley AF. A quantitative description of membrane current and its application to conduction and excitation in nerve. *J Physiol* 1952, 117:500–544.
32. McAllister RE, Noble D, Tsien RW. Reconstruction of the electrical activity of cardiac Purkinje fibres. *J Physiol* 1975, 251:1–59.
33. Noble D. The surprising heart: a review of recent progress in cardiac electrophysiology. *J Physiol* 1984, 353:1–50.
34. Beeler GW, Reuter H. Reconstruction of the action potential of ventricular myocardial fibres. *J Physiol* 1977, 268:177–210.
35. DiFrancesco D, Noble D. A model of cardiac electrical activity incorporating ionic pumps and concentration changes. *Phil Trans R Soc Lond B Biol Sci* 1985, 307:353–398.
36. Noble D, Noble SJ. A model of sino-atrial node electrical activity based on a modification of the DiFrancesco-Noble (1984) equations. *Proc R Soc Lond B Biol Sci* 1984, 222:295–304.
37. Noble D, DiFrancesco D, Denyer J. Ionic mechanisms in normal and abnormal cardiac pacemaker activity. In: Jacklet JW, ed. *Cellular and Neuronal Oscillators*. New York: Dekker; 1989, 59–85.
38. Earm YE, Noble D. A model of the single atrial cell: relation between calcium current and calcium release. *Proc R Soc Lond B Biol Sci* 1990, 240:83–96.
39. Noble D, Denyer JC, Brown HF, DiFrancesco D. Reciprocal role of the inward currents ib, Na and i(f) in controlling and stabilizing pacemaker frequency of rabbit sino-atrial node cells. *Proc Biol Sci* 1992, 250:199–207.
40. Hilgemann DW, Noble D. Excitation–contraction coupling and extracellular calcium transients in rabbit atrium: reconstruction of basic cellular mechanisms. *Proc R Soc Lond B Biol Sci* 1987, 230:163–205.
41. Wilders R. Computer modelling of the sinoatrial node. *Med Biol Eng Comput* 2007, 45:189–207.

42. Demir SS, Clark JW, Murphey CR, Giles WR. A mathematical model of a rabbit sinoatrial node cell. *Am J Physiol* 1994, 266:C832–C852.
43. Dokos S, Celler B, Lovell N. Ion currents underlying sinoatrial node pacemaker activity: a new single cell mathematical model. *J Theor Biol* 1996, 181:245–272.
44. Zhang H, Holden AV, Kodama I, Honjo H, Lei M, Varghese T, Boyett MR. Mathematical models of action potentials in the periphery and center of the rabbit sinoatrial node. *Am J Physiol Heart Circ Physiol* 2000, 279:H397–H421.
45. Zhang H, Holden AV, Boyett MR. Gradient model versus mosaic model of the sinoatrial node. *Circulation* 2001, 103:584–588.
46. Lovell NH, Cloherty SL, Celler BG, Dokos S. A gradient model of cardiac pacemaker myocytes. *Prog Biophys Mol Biol* 2004, 85:301–323.
47. Maltsev VA, Vinogradova TM, Bogdanov KY, Lakatta EG, Stern MD. Diastolic calcium release controls the beating rate of rabbit sinoatrial node cells: numerical modeling of the coupling process. *Biophys J* 2004, 86:2596–2605.
48. Vinogradova TM, Zhou YY, Maltsev V, Lyashkov A, Stern M, Lakatta EG. Rhythmic ryanodine receptor Ca2+ releases during diastolic depolarization of sinoatrial pacemaker cells do not require membrane depolarization. *Circ Res* 2004, 94:802–809.
49. Nygren A, Fiset C, Firek L, Clark JW, Lindblad DS, Clark RB, Giles WR. Mathematical model of an adult human atrial cell: the role of K+ currents in repolarization. *Circ Res* 1998, 82:63–81.
50. Courtemanche M, Ramirez RJ, Nattel S. Ionic mechanisms underlying human atrial action potential properties: insights from a mathematical model. *Am J Physiol* 1998, 275:H301–H321.
51. Inada S, Hancox JC, Zhang H, Boyett MR. One-dimensional mathematical model of the atrioventricular node including atrio-nodal, nodal, and nodal-his cells. *Biophys J* 2009, 97:2117–2127.
52. Stewart P, Aslanidi OV, Noble D, Noble PJ, Boyett MR, Zhang H. Mathematical models of the electrical action potential of Purkinje fibre cells. *Phil Trans A Math Phys Eng Sci* 2009, 367:2225–2255.
53. Yanagihara K, Noma A, Irisawa H. Reconstruction of sino-atrial node pacemaker potential based on the voltage clamp experiments. *Jpn J Physiol* 1980, 30:841–857.
54. Bristow DG, Clark JW. A mathematical model of primary pacemaking cell in SA node of the heart. *Am J Physiol* 1982, 243:H207–H218.
55. Irisawa H, Noma A. Pacemaker mechanisms of rabbit sinoatrial node cells. In: Bouman L, Jongsma H, eds. *Cardiac Rate and Rhythm: Physiological, Morphological, and Developmental Aspects*. London: Martinus Nijhoff; 1982, 35–51.
56. Rasmusson RL, Clark JW, Giles WR, Shibata EF, Campbell DL. A mathematical model of a bullfrog cardiac pacemaker cell. *Am J Physiol* 1990, 259:H352–H369.
57. Wilders R, Jongsma HJ, van Ginneken AC. Pacemaker activity of the rabbit sinoatrial node. A comparison of mathematical models. *Biophys J* 1991, 60:1202–1216.
58. Dokos S, Celler BG, Lovell NH. Modification of DiFrancesco-Noble equations to simulate the effects of vagal stimulation on in vivo mammalian sinoatrial node electrical activity. *Ann Biomed Eng* 1993, 21:321–335.
59. Endresen LP, Hall K, Hoye JS, Myrheim J. A theory for the membrane potential of living cells. *Eur Biophys J* 2000, 29:90–103.
60. Kurata Y, Hisatome I, Imanishi S, Shibamoto T. Dynamical description of sinoatrial node pacemaking: improved mathematical model for primary pacemaker cell. *Am J Physiol Heart Circ Physiol* 2002, 283:H2074–H2101.
61. Garny A, Kohl P, Hunter PJ, Boyett MR, Noble D. One-dimensional rabbit sinoatrial node models: benefits and limitations. *J Cardiovasc Electrophysiol* 2003, 14(suppl):S121–S132.
62. Sarai N, Matsuoka S, Kuratomi S, Ono K, Noma A. Role of individual ionic current systems in the SA node hypothesized by a model study. *Jpn J Physiol* 2003, 53:125–134.
63. Mangoni ME, Traboulsie A, Leoni AL, Couette B, Marger L, Le Quang K, Kupfer E, Cohen-Solal A, Vilar J, Shin HS, et al. Bradycardia and slowing of the atrioventricular conduction in mice lacking CaV3.1/alpha1G T-type calcium channels. *Circ Res* 2006, 98:1422–1430.
64. Maltsev VA, Lakatta EG. Synergism of coupled subsarcolemmal Ca2+ clocks and sarcolemmal voltage clocks confers robust and flexible pacemaker function in a novel pacemaker cell model. *Am J Physiol Heart Circ Physiol* 2009, 296:H594–H615.
65. Lindblad DS, Murphey CR, Clark JW, Giles WR. A model of the action potential and underlying membrane currents in a rabbit atrial cell. *Am J Physiol* 1996, 271:H1666–H1696.
66. Ramirez RJ, Nattel S, Courtemanche M. Mathematical analysis of canine atrial action potentials: rate, regional factors, and electrical remodeling. *Am J Physiol Heart Circ Physiol* 2000, 279: H1767–H1785.
67. Aslanidi OV, Boyett MR, Dobrzynski H, Li J, Zhang H. Mechanisms of transition from normal to reentrant electrical activity in a model of rabbit atrial tissue: interaction of tissue heterogeneity and anisotropy. *Biophys J* 2009, 96:798–817.
68. Maleckar MM, Greenstein JL, Giles WR, Trayanova NA. K+ current changes account for the rate

dependence of the action potential in the human atrial myocyte. *Am J Physiol Heart Circ Physiol* 2009, 297:H1398–H1410.

69. Liu Y, Zeng W, Delmar M, Jalife J. Ionic mechanisms of electronic inhibition and concealed conduction in rabbit atrioventricular nodal myocytes. *Circulation* 1993, 88:1634–1646.
70. Noble D, Noble S, Bett G, Earm YE, Ko WK, So IK. The role of sodium-calcium exchange during the cardiac action potential. *Ann N Y Acad Sci* 1991, 639:334–354.
71. Luo CH, Rudy Y. A model of the ventricular cardiac action potential. Depolarization, repolarization, and their interaction. *Circ Res* 1991, 68:1501–1526.
72. Nordin C. Computer model of membrane current and intracellular Ca2+ flux in the isolated guinea pig ventricular myocyte. *Am J Physiol* 1993, 265:H2117–H2136.
73. Luo CH, Rudy Y. A dynamic model of the cardiac ventricular action potential. I. Simulations of ionic currents and concentration changes. *Circ Res* 1994, 74:1071–1096.
74. Luo CH, Rudy Y. A dynamic model of the cardiac ventricular action potential. II. Afterdepolarizations, triggered activity, and potentiation. *Circ Res* 1994, 74:1097–1113.
75. Jafri MS, Rice JJ, Winslow RL. Cardiac Ca2+ dynamics: the roles of ryanodine receptor adaptation and sarcoplasmic reticulum load. *Biophys J* 1998, 74:1149–1168.
76. Noble D, Varghese A, Kohl P, Noble P. Improved guinea-pig ventricular cell model incorporating a diadic space, IKr and IKs, and length- and tension-dependent processes. *Can J Cardiol* 1998, 14:123–134.
77. Priebe L, Beuckelmann DJ. Simulation study of cellular electric properties in heart failure. *Circ Res* 1998, 82:1206–1223.
78. Winslow RL, Rice J, Jafri S, Marban E, O'Rourke B. Mechanisms of altered excitation–contraction coupling in canine tachycardia-induced heart failure, II: model studies. *Circ Res* 1999, 84:571–586.
79. Pandit SV, Clark RB, Giles WR, Demir SS. A mathematical model of action potential heterogeneity in adult rat left ventricular myocytes. *Biophys J* 2001, 81:3029–3051.
80. Hund TJ, Kucera JP, Otani NF, Rudy Y. Ionic charge conservation and long-term steady state in the Luo-Rudy dynamic cell model. *Biophys J* 2001, 81:3324–3331.
81. Puglisi JL, Bers DM. LabHEART: an interactive computer model of rabbit ventricular myocyte ion channels and Ca transport. *Am J Physiol Cell Physiol* 2001, 281:C2049–C2060.
82. Bernus O, Wilders R, Zemlin CW, Verschelde H, Panfilov AV. A computationally efficient electrophysiological model of human ventricular cells. *Am J Physiol Heart Circ Physiol* 2002, 282:H2296–H2308.
83. Fox JJ, McHarg JL, Gilmour RF Jr. Ionic mechanism of electrical alternans. *Am J Physiol Heart Circ Physiol* 2002, 282:H516–H530.
84. Greenstein JL, Winslow RL. An integrative model of the cardiac ventricular myocyte incorporating local control of Ca2+ release. *Biophys J* 2002, 83:2918–2945.
85. Cabo C, Boyden PA. Electrical remodeling of the epicardial border zone in the canine infarcted heart: a computational analysis. *Am J Physiol Heart Circ Physiol* 2003, 284:H372–H384.
86. Matsuoka S, Sarai N, Kuratomi S, Ono K, Noma A. Role of individual ionic current systems in ventricular cells hypothesized by a model study. *Jpn J Physiol* 2003, 53:105–123.
87. Iyer V, Mazhari R, Winslow RL. A computational model of the human left-ventricular epicardial myocyte. *Biophys J* 2004, 87:1507–1525.
88. Matsuoka S, Sarai N, Jo H, Noma A. Simulation of ATP metabolism in cardiac excitation–contraction coupling. *Prog Biophys Mol Biol* 2004, 85:279–299.
89. Bondarenko VE, Szigeti GP, Bett GC, Kim SJ, Rasmusson RL. Computer model of action potential of mouse ventricular myocytes. *Am J Physiol Heart Circ Physiol* 2004, 287:H1378–H1403.
90. Shannon TR, Wang F, Puglisi J, Weber C, Bers DM. A mathematical treatment of integrated Ca dynamics within the ventricular myocyte. *Biophys J* 2004, 87:3351–3371.
91. ten Tusscher KH, Noble D, Noble PJ, Panfilov AV. A model for human ventricular tissue. *Am J Physiol Heart Circ Physiol* 2004, 286:H1573–H1589.
92. Hund TJ, Rudy Y. Rate dependence and regulation of action potential and calcium transient in a canine cardiac ventricular cell model. *Circulation* 2004, 110:3168–3174.
93. Greenstein JL, Hinch R, Winslow RL. Mechanisms of excitation–contraction coupling in an integrative model of the cardiac ventricular myocyte. *Biophys J* 2006, 90:77–91.
94. Cortassa S, Aon MA, O'Rourke B, Jacques R, Tseng HJ, Marban E, Winslow RL. A computational model integrating electrophysiology, contraction, and mitochondrial bioenergetics in the ventricular myocyte. *Biophys J* 2006, 91:1564–1589.
95. Crampin EJ, Smith NP. A dynamic model of excitation–contraction coupling during acidosis in cardiac ventricular myocytes. *Biophys J* 2006, 90:3074–3090.

96. Crampin EJ, Smith NP, Langham AE, Clayton RH, Orchard CH. Acidosis in models of cardiac ventricular myocytes. *Phil Trans A Math Phys Eng Sci* 2006, 364:1171–1186.
97. Mahajan A, Shiferaw Y, Sato D, Baher A, Olcese R, Xie LH, Yang MJ, Chen PS, Restrepo JG, Karma A, et al. A rabbit ventricular action potential model replicating cardiac dynamics at rapid heart rates. *Biophys J* 2008, 94:392–410.
98. Pasek M, Simurda J, Orchard CH, Christe G. A model of the guinea-pig ventricular cardiac myocyte incorporating a transverse-axial tubular system. *Prog Biophys Mol Biol* 2008, 96:258–280.
99. Faber GM, Rudy Y. Action potential and contractility changes in [Na(+)](i) overloaded cardiac myocytes: a simulation study. *Biophys J* 2000, 78:2392–2404.
100. Wang LJ, Sobie EA. Mathematical model of the neonatal mouse ventricular action potential. *Am J Physiol Heart Circ Physiol* 2008, 294:H2565–H2575.
101. Hashambhoy YL, Winslow RL, Greenstein JL. CaMKII-induced shift in modal gating explains L-type Ca(2+) current facilitation: a modeling study. *Biophys J* 2009, 96:1770–1785.
102. Korhonen T, Rapila R, Tavi P. Mathematical model of mouse embryonic cardiomyocyte excitation–contraction coupling. *J Gen Physiol* 2008, 132:407–419.
103. Korhonen T, Hanninen SL, Tavi P. Model of excitation–contraction coupling of rat neonatal ventricular myocytes. *Biophys J* 2009, 96:1189–1209.
104. Grandi E, Pasqualini FS, Bers DM. A novel computational model of the human ventricular action potential and Ca transient. *J Mol Cell Cardiol* 2010, 48:112–121.
105. Koivumaki JT, Korhonen T, Takalo J, Weckstrom M, Tavi P. Regulation of excitation–contraction coupling in mouse cardiac myocytes: integrative analysis with mathematical modelling. *BMC Physiol* 2009, 9:16.
106. Hoel PG, Port SC, Stone CJ. *Introduction to Stochastic Processes*. Boston, MA: Houghton Mifflin; 1972.
107. Hille B. *Ionic Channels of Excitable Membranes*. 2nd ed. Sundeland: Sinauer; 1992, 341–345.
108. Chay TR. The Hodgkin-Huxley Na+ channel model versus the five-state Markovian model. *Biopolymers* 1991, 31:1483–1502.
109. Horn R, Vandenberg CA. Statistical properties of single sodium channels. *J Gen Physiol* 1984, 84:505–534.
110. Mazhari R, Greenstein JL, Winslow RL, Marban E, Nuss HB. Molecular interactions between two long-QT syndrome gene products, HERG and KCNE2, rationalized by in vitro and in silico analysis. *Circ Res* 2001, 89:33–38.
111. Vecchietti S, Rivolta I, Severi S, Napolitano C, Priori SG, Cavalcanti S. Computer simulation of wild-type and mutant human cardiac Na+ current. *Med Biol Eng Comput* 2006, 44:35–44.
112. Vecchietti S, Grandi E, Severi S, Rivolta I, Napolitano C, Priori SG, Cavalcanti S. In silico assessment of Y1795C and Y1795H SCN5A mutations: implication for inherited arrhythmogenic syndromes. *Am J Physiol Heart Circ Physiol* 2007, 292:H56–H65.
113. Clancy CE, Rudy Y. Cellular consequences of HERG mutations in the long QT syndrome: precursors to sudden cardiac death. *Cardiovasc Res* 2001, 50:301–313.
114. Clancy CE, Rudy Y. Linking a genetic defect to its cellular phenotype in a cardiac arrhythmia. *Nature* 1999, 400:566–569.
115. Brennan T, Fink M, Rodriguez B, tarassenko L. Modeling effects of sotalol on action potential morphology using a novel Markov model of HERG channel, Paper presented at MEDICON, IFMB Proceedings, 2007.
116. Brennan T, Stokely D, Fink M, Rodriguez B, Tarassenko L. Modeling the effects of sotalol on T-wave morphology. *Comput Cardiol IEEE* 2007, 34:249–252.
117. Clancy CE, Zhu ZI, Rudy Y. Pharmacogenetics and anti-arrhythmic drug therapy: a theoretical investigation. *Am J Physiol Heart Circ Physiol* 2007, 292:H66–H75.
118. Brennan T, Fink M, Rodriguez B. Multiscale modelling of drug-induced effects on cardiac electrophysiological activity. *Eur J Pharm Sci* 2009, 36:62–77.
119. Grandi E, Puglisi JL, Wagner S, Maier LS, Severi S, Bers DM. Simulation of Ca-calmodulin-dependent protein kinase II on rabbit ventricular myocyte ion currents and action potentials. *Biophys J* 2007, 93:3835–3847.
120. Irvine LA, Jafri MS, Winslow RL. Cardiac sodium channel Markov model with temperature dependence and recovery from inactivation. *Biophys J* 1999, 76:1868–1885.
121. Oehmen CS, Giles WR, Demir SS. Mathematical model of the rapidly activating delayed rectifier potassium current I(Kr) in rabbit sinoatrial node. *J Cardiovasc Electrophysiol* 2002, 13:1131–1140.
122. Fink M, Noble D, Virag L, Varro A, Giles WR. Contributions of HERG K+ current to repolarization of the human ventricular action potential. *Prog Biophys Mol Biol* 2008, 96:357–376.
123. Bondarenko VE, Bett GC, Rasmusson RL. A model of graded calcium release and L-type Ca2+ channel inactivation in cardiac muscle. *Am J Physiol Heart Circ Physiol* 2004, 286:H1154–H1169.
124. Shannon TR, Ginsburg KS, Bers DM. Reverse mode of the sarcoplasmic reticulum Ca pump limits sarcoplasmic reticulum Ca uptake in permeabilized and voltage-clamped myocytes. *Ann N Y Acad Sci* 1998, 853:350–352.

125. Smith NP, Crampin EJ. Development of models of active ion transport for whole-cell modelling: cardiac sodium-potassium pump as a case study. *Prog Biophys Mol Biol* 2004, 85:387–405.

126. Tran K, Smith NP, Loiselle DS, Crampin EJ. A thermodynamic model of the cardiac sarcoplasmic/endoplasmic Ca(2+) (SERCA) pump. *Biophys J* 2009, 96:2029–2042.

127. Leem CH, Lagadic-Gossmann D, Vaughan-Jones RD. Characterization of intracellular pH regulation in the guinea-pig ventricular myocyte. *J Physiol* 1999, 517:159–180.

128. Bers D, Stiffel V. Ratio of ryanodine to dihydropyridine receptors in cardiac and skeletal muscle and implications for E-C coupling. *Am J Physiol* 1993, 264:C1587–C1593.

129. Fabiato A. Time and calcium dependence of activation and inactivation of calcium-induced release of calcium from the sarcoplasmic reticulum of a skinned canine cardiac Purkinje cell. *J Gen Physiol* 1985, 85:247–289.

130. Alseikhan BA, DeMaria CD, Colecraft HM, Yue DT. Engineered calmodulins reveal the unexpected eminence of Ca2+ channel inactivation in controlling heart excitation. *Proc Natl Acad Sci U S A* 2002, 99:17185–17190.

131. Stern MD. Theory of excitation–contraction coupling in cardiac muscle. *Biophys J* 1992, 63:497–517.

132. Stern MD, Lakatta EG. Excitation–contraction coupling in the heart: the state of the question. *FASEB J* 1992, 6:3092–3100.

133. Cheng H, Lederer WJ, Cannell MB. Calcium sparks: elementary events underlying excitation–contraction coupling in heart muscle. *Science* 1993, 262:740–744.

134. Tanskanen A, Winslow RL. Integrative, structurally-detailed model of calcium dynamics in the cardiac diad. *SIAM J Multiscale Model Simul* 2006, 5:1280–1296.

135. Hinch R, Greenstein JL, Winslow RL. Multi-scale models of local control of calcium induced calcium release. *Prog Biophys Mol Biol* 2006, 90:136–150.

136. Hinch R, Greenstein JL, Tanskanen AJ, Xu L, Winslow RL. A simplified local control model of calcium-induced calcium release in cardiac ventricular myocytes. *Biophys J* 2004, 87:3723–3736.

137. Flaim SN, Giles WR, McCulloch AD. Contributions of sustained INa and IKv43 to transmural heterogeneity of early repolarization and arrhythmogenesis in canine left ventricular myocytes. *Am J Physiol Heart Circ Physiol* 2006, 291:H2617–H2629.

138. Altamirano J, Bers DM. Voltage dependence of cardiac excitation–contraction coupling: unitary Ca2+ current amplitude and open channel probability. *Circ Res* 2007, 101:590–597.

139. Trafford AW, Diaz ME, O'Neill SC, Eisner DA. Comparison of subsarcolemmal and bulk calcium concentration during spontaneous calcium release in rat ventricular myocytes. *J Physiol* 1995, 488:577–586.

140. Stern MD, Song LS, Cheng H, Sham JS, Yang HT, Boheler KR, Rios E. Local control models of cardiac excitation–contraction coupling. A possible role for allosteric interactions between ryanodine receptors. *J Gen Physiol* 1999, 113:469–489.

141. Bassani JW, Yuan W, Bers DM. Fractional SR Ca release is regulated by trigger Ca and SR Ca content in cardiac myocytes. *Am J Physiol* 1995, 268:C1313–C1319.

142. Eisner DA, Trafford AW, Diaz ME, Overend CL, O'Neill SC. The control of Ca release from the cardiac sarcoplasmic reticulum: regulation versus autoregulation. *Cardiovasc Res* 1998, 38:589–604.

143. Shannon TR, Wang F, Bers DM. Regulation of cardiac sarcoplasmic reticulum Ca release by luminal [Ca] and altered gating assessed with a mathematical model. *Biophys J* 2005, 89:4096–4110.

144. Stevens SC, Terentyev D, Kalyanasundaram A, Periasamy M, Gyorke S. Intra-sarcoplasmic reticulum Ca2+ oscillations are driven by dynamic regulation of ryanodine receptor function by luminal Ca2+ in cardiomyocytes. *J Physiol* 2009, 587:4863–4872.

145. Zima AV, Picht E, Bers DM, Blatter LA. Termination of cardiac Ca2+ sparks: role of intra-SR [Ca2+], release flux, and intra-SR Ca2+ diffusion. *Circ Res* 2008, 103:e105–e115.

146. Zima AV, Picht E, Bers DM, Blatter LA. Partial inhibition of sarcoplasmic reticulum ca release evokes long-lasting ca release events in ventricular myocytes: role of luminal ca in termination of ca release. *Biophys J* 2008, 94:1867–1879.

147. Achs MJ, Garfinkel D. Computer simulation of energy metabolism in anoxic perfused rat heart. *Am J Physiol* 1977, 232:R164–R174.

148. Achs MJ, Garfinkel D. Computer simulation of rat heart metabolism after adding glucose to the perfusate. *Am J Physiol* 1977, 232:R175–R184.

149. Kohn MC, Garfinkel D. Computer simulation of ischemic rat heart purine metabolism. I. Model construction. *Am J Physiol* 1977, 232:H386–H393.

150. Achs MJ, Garfinkel D. Metabolism of the acutely ischemic dog heart. I. Construction of a computer model. *Am J Physiol* 1979, 236:R21–R30.

151. Kohn MC, Achs MJ, Garfinkel D. Computer simulation of metabolism in pyruvate-perfused rat heart. I. Model construction. *Am J Physiol* 1979, 237:R153–R158.

152. Kohn MC, Garfinkel D. Computer simulation of metabolism in palmitate-perfused rat heart. I. Palmitate oxidation. *Ann Biomed Eng* 1983, 11:361–384.

153. Kohn MC. Computer simulation of metabolism in palmitate-perfused rat heart. III. Sensitivity analysis. *Ann Biomed Eng* 1983, 11:533–549.

154. Chance B, Williams GR. The respiratory chain and oxidative phosphorylation. *Adv Enzymol Relat Subj Biochem* 1956, 17:65–134.

155. Balaban RS, Heineman FW. Control of mitochondrial respiration in the heart in vivo. *Mol Cell Biochem* 1989, 89:191–197.

156. Saks VA, Kaambre T, Sikk P, Eimre M, Orlova E, Paju K, Piirsoo A, Appaix F, Kay L, Regitz-Zagrosek V, et al. Intracellular energetic units in red muscle cells. *Biochem J* 2001, 356:643–657.

157. Vendelin M, Kongas O, Saks V. Regulation of mitochondrial respiration in heart cells analyzed by reaction-diffusion model of energy transfer. *Am J Physiol Cell Physiol* 2000, 278:C747–C764.

158. Saks V, Kuznetsov A, Andrienko T, Usson Y, Appaix F, Guerrero K, Kaambre T, Sikk P, Lemba M, Vendelin M. Heterogeneity of ADP diffusion and regulation of respiration in cardiac cells. *Biophys J* 2003, 84:3436–3456.

159. van Beek JH, van Wijhe MH, Eijgelshoven MH, Hak JB. Dynamic adaptation of cardiac oxidative phosphorylation is not mediated by simple feedback control. *Am J Physiol* 1999, 277:H1375–H1384.

160. Kongas O, van Beek JH. Diffusion barriers for ADP in the cardiac cell. *Mol Biol Rep* 2002, 29:141–144.

161. van Beek JH. Adenine nucleotide-creatine-phosphate module in myocardial metabolic system explains fast phase of dynamic regulation of oxidative phosphorylation. *Am J Physiol Cell Physiol* 2007, 293:C815–C829.

162. Ch'en FF, Vaughan-Jones RD, Clarke K, Noble D. Modelling myocardial ischaemia and reperfusion. *Prog Biophys Mol Biol* 1998, 69:515–538.

163. Swietach P, Leem CH, Spitzer KW, Vaughan-Jones RD. Experimental generation and computational modeling of intracellular pH gradients in cardiac myocytes. *Biophys J* 2005, 88:3018–3037.

164. Korzeniewski B, Mazat JP. Theoretical studies on the control of oxidative phosphorylation in muscle mitochondria: application to mitochondrial deficiencies. *Biochem J* 1996, 319:143–148.

165. Cortassa S, Aon MA, Marban E, Winslow RL, O'Rourke B. An integrated model of cardiac mitochondrial energy metabolism and calcium dynamics. *Biophys J* 2003, 84:2734–2755.

166. Hafner RP, Brown GC, Brand MD. Analysis of the control of respiration rate, phosphorylation rate, proton leak rate and protonmotive force in isolated mitochondria using the 'top-down' approach of metabolic control theory. *Eur J Biochem* 1990, 188:313–319.

167. Brandes R, Bers DM. Simultaneous measurements of mitochondrial NADH and Ca(2+) during increased work in intact rat heart trabeculae. *Biophys J* 2002, 83:587–604.

168. Nguyen MH, Jafri MS. Mitochondrial calcium signaling and energy metabolism. *Ann N Y Acad Sci* 2005, 1047:127–137.

169. Trollinger DR, Cascio WE, Lemasters JJ. Mitochondrial calcium transients in adult rabbit cardiac myocytes: inhibition by ruthenium red and artifacts caused by lysosomal loading of Ca(2+)-indicating fluorophores. *Biophys J* 2000, 79:39–50.

170. Beard DA. A biophysical model of the mitochondrial respiratory system and oxidative phosphorylation. *PLoS Comput Biol* 2005, 1:e36.

171. Wu F, Yang F, Vinnakota KC, Beard DA. Computer modeling of mitochondrial tricarboxylic acid cycle, oxidative phosphorylation, metabolite transport, and electrophysiology. *J Biol Chem* 2007, 282:24525–24537.

172. Jo H, Noma A, Matsuoka S. Calcium-mediated coupling between mitochondrial substrate dehydrogenation and cardiac workload in single guinea-pig ventricular myocytes. *J Mol Cell Cardiol* 2006, 40:394–404.

173. Rice JJ, Jafri MS, Winslow RL. Modeling short-term interval-force relations in cardiac muscle. *Am J Physiol Heart Circ Physiol* 2000, 278:H913–H931.

174. Maack C, Cortassa S, Aon MA, Ganesan AN, Liu T, O'Rourke B. Elevated cytosolic Na+ decreases mitochondrial Ca2+ uptake during excitation–contraction coupling and impairs energetic adaptation in cardiac myocytes. *Circ Res* 2006, 99:172–182.

175. Elliott AC, Smith GL, Allen DG. The metabolic consequences of an increase in the frequency of stimulation in isolated ferret hearts. *J Physiol* 1994, 474:147–159.

176. Cortassa S, O'Rourke B, Winslow RL, Aon MA. Control and regulation of mitochondrial energetics in an integrated model of cardiomyocyte function. *Biophys J* 2009, 96:2466–2478.

177. Cortassa S, Aon MA, Winslow RL, O'Rourke B. A mitochondrial oscillator dependent on reactive oxygen species. *Biophys J* 2004, 87:2060–2073.

178. Aon MA, Cortassa S, Marban E, O'Rourke B. Synchronized whole cell oscillations in mitochondrial metabolism triggered by a local release of reactive oxygen species in cardiac myocytes. *J Biol Chem* 2003, 278:44735–44744.

179. Aon MA, Cortassa S, O'Rourke B. Percolation and criticality in a mitochondrial network. *Proc Natl Acad Sci U S A* 2004, 101:4447–4452.

180. Zhou L, Aon MA, Almas T, Cortassa S, Winslow RL, O'Rourke B. A reaction-diffusion model of ROS-induced ROS release in a mitochondrial network. *PLoS Comput Biol* 2010, 6:e1000657.

181. Zhou L, Trayanova N, Plank G, Aon MA, Cortassa S, O'Rourke B. Effects of mitochondrial depolarization on cardiac electrical activity in an integrated

multiscale model of the myocardium. *Biophys J* 2009, 96(suppl 1): 663a–664a.

182. Rice JJ, Wang F, Bers DM, de Tombe PP. Approximate model of cooperative activation and crossbridge cycling in cardiac muscle using ordinary differential equations. *Biophys J* 2008, 95:2368–2390.
183. Rice JJ, de Tombe PP. Approaches to modeling crossbridges and calcium-dependent activation in cardiac muscle. *Prog Biophys Mol Biol* 2004, 85:179–195.
184. Bers DM. *Excitation–contraction Coupling and Cardiac Contractile Force*. 2nd ed. Boston, MA: Kluwer; 2001.
185. Dobesh DP, Konhilas JP, de Tombe PP. Cooperative activation in cardiac muscle: Impact of sarcomere length. *Am J Physiol Heart Circ Physiol* 2002, 282:H1055–H1062.
186. Hunter PJ, McCulloch AD, ter Keurs HE. Modelling the mechanical properties of cardiac muscle. *Prog Biophys Mol Biol* 1998, 69:289–331.
187. Landesberg A, Sideman S. Coupling calcium binding to troponin C and cross-bridge cycling in skinned cardiac cells. *Am J Physiol* 1994, 266:H1260–H1271.
188. Rice JJ, Winslow RL, Hunter WC. Comparison of putative cooperative mechanisms in cardiac muscle: length dependence and dynamic responses. *Am J Physiol* 1999, 276:H1734–H1754.
189. Razumova MV, Bukatina AE, Campbell KB. Stiffness-distortion sarcomere model for muscle simulation. *J Appl Physiol* 1999, 87:1861–1876.
190. Negroni JA, Lascano EC. Concentration and elongation of attached cross-bridges as pressure determinants in a ventricular model. *J Mol Cell Cardiol* 1999, 31:1509–1526.
191. Smith NP. From sarcomere to cell: an efficient algorithm for linking mathematical models of muscle contraction. *Bull Math Biol* 2003, 65:1141–1162.
192. Campbell KB, Razumova MV, Kirkpatrick RD, Slinker BK. Myofilament kinetics in isometric twitch dynamics. *Ann Biomed Eng* 2001, 29:384–405.
193. Izakov V, Katsnelson LB, Blyakhman FA, Markhasin VS, Shklyar TF. Cooperative effects due to calcium binding by troponin and their consequences for contraction and relaxation of cardiac muscle under various conditions of mechanical loading. *Circ Res* 1991, 69:1171–1184.
194. Niederer SA, Hunter PJ, Smith NP. A quantitative analysis of cardiac myocyte relaxation: a simulation study. *Biophys J* 2006, 90:1697–1722.
195. Niederer SA, Smith NP. A mathematical model of the slow force response to stretch in rat ventricular myocytes. *Biophys J* 2007, 92:4030–4044.
196. Niederer SA, Smith NP. The role of the Frank-Starling law in the transduction of cellular work to whole organ pump function: a computational modeling analysis. *PLoS Comput Biol* 2009, 5:e1000371.
197. Campbell SG, Flaim SN, Leem CH, McCulloch AD. Mechanisms of transmurally varying myocyte electromechanics in an integrated computational model. *Phil Trans A Math Phys Eng Sci* 2008, 366:3361–3380.
198. Campbell SG, Howard E, Aguado-Sierra J, Coppola BA, Omens JH, Mulligan LJ, McCulloch AD, Kerckhoffs RC. Effect of transmurally heterogeneous myocyte excitation–contraction coupling on canine left ventricular electromechanics. *Exp Physiol* 2009, 94:541–552.
199. Tran K, Smith NP, Loiselle DS, Crampin EJ. A metabolite-sensitive, thermodynamically constrained model of cardiac cross-bridge cycling: implications for force development during ischemia. *Biophys J* 2010, 98:267–276.
200. El-Armouche A, Eschenhagen T. Beta-adrenergic stimulation and myocardial function in the failing heart. *Heart Fail Rev* 2009, 14:225–241.
201. Bers DM. Calcium cycling and signaling in cardiac myocytes. *Annu Rev Physiol* 2008, 70:23–49.
202. Greenstein JL, Tanskanen AJ, Winslow RL. Modeling the actions of beta-adrenergic signaling on excitation–contraction coupling processes. *Ann N Y Acad Sci* 2004, 1015:16–27.
203. Tanskanen AJ, Greenstein JL, O'Rourke B, Winslow RL. The role of stochastic and modal gating of cardiac L-type Ca2+ channels on early after-depolarizations. *Biophys J* 2005, 88:85–95.
204. Saucerman JJ, Brunton LL, Michailova AP, McCulloch AD. Modeling beta-adrenergic control of cardiac myocyte contractility in silico. *J Biol Chem* 2003, 278:47997–48003.
205. Ahrens-Nicklas RC, Clancy CE, Christini DJ. Re-evaluating the efficacy of β-adrenergic agonists and antagonists in long QT-3 syndrome through computational modelling. *Cardiovasc Res* 2009, 82:439–447.
206. Maier LS, Bers DM. Role of Ca2+/calmodulin-dependent protein kinase (CaMK) in excitation–contraction coupling in the heart. *Cardiovasc Res* 2007, 73:631–640.
207. Currie S, Loughrey CM, Craig MA, Smith GL. Calcium/calmodulin-dependent protein kinase IIdelta associates with the ryanodine receptor complex and regulates channel function in rabbit heart. *Biochem J* 2004, 377:357–366.
208. Hudmon A, Schulman H, Kim J, Maltez JM, Tsien RW, Pitt GS. CaMKII tethers to L-type Ca2+ channels, establishing a local and dedicated integrator of Ca2+ signals for facilitation. *J Cell Biol* 2005, 171:537–547.
209. Ai X, Curran JW, Shannon TR, Bers DM, Pogwizd SM. Ca2+/calmodulin-dependent protein kinase modulates cardiac ryanodine receptor phosphorylation and sarcoplasmic reticulum Ca2+ leak in heart failure. *Circ Res* 2005, 97:1314–1322.

210. Hudmon A, Schulman H. Structure-function of the multifunctional Ca2+/calmodulin-dependent protein kinase II. *Biochem J* 2002, 364:593–611.

211. Wagner S, Dybkova N, Rasenack EC, Jacobshagen C, Fabritz L, Kirchhof P, Maier SK, Zhang T, Hasenfuss G, Brown JH, et al. Ca2+/calmodulin-dependent protein kinase II regulates cardiac Na+ channels. *J Clin Invest* 2006, 116:3127–3138.

212. Saucerman JJ, Bers DM. Calmodulin mediates differential sensitivity of CaMKII and calcineurin to local Ca2+ in cardiac myocytes. *Biophys J* 2008, 95:4597–4612.

213. Hashambhoy YL, Greenstein JL, Winslow RL. Role of CaMKII in RyR leak, EC coupling and action potential duration: a computational model. *J Mol Cell Cardiol* 2010, 49:617–624.

214. Silva JR, Pan H, Wu D, Nekouzadeh A, Decker KF, Cui J, Baker NA, Sept D, Rudy Y. A multiscale model linking ion-channel molecular dynamics and electrostatics to the cardiac action potential. *Proc Natl Acad Sci U S A* 2009, 106:11102–11106.

215. Marx SO, Reiken S, Hisamatsu Y, Jayaraman T, Burkhoff D, Rosemblit N, Marks AR. PKA phosphorylation dissociates FKBP12.6 from the calcium release channel (ryanodine receptor): defective regulation in failing hearts. *Cell* 2000, 101:365–376.

216. Shannon TR, Pogwizd SM, Bers DM. Elevated sarcoplasmic reticulum Ca2+ leak in intact ventricular myocytes from rabbits in heart failure. *Circ Res* 2003, 93:592–594.

217. Yano M, Yamamoto T, Ikeda Y, Matsuzaki M. Mechanisms of Disease: ryanodine receptor defects in heart failure and fatal arrhythmia. *Nat Clin Pract Cardiovasc Med* 2006, 3:43–52.